



UNIVERSITY OF LEEDS

This is a repository copy of *The Effect of Improper Curing on Properties That May Affect Concrete Durability*.

White Rose Research Online URL for this paper:
<http://eprints.whiterose.ac.uk/120196/>

Version: Accepted Version

Article:

Idowu, O and Black, L orcid.org/0000-0001-8531-4989 (2018) The Effect of Improper Curing on Properties That May Affect Concrete Durability. *Magazine of Concrete Research*, 70 (12). pp. 633-647. ISSN 0024-9831

<https://doi.org/10.1680/jmacr.17.00148>

© ICE Publishing. This is an author produced version of a paper published in *Magazine of Concrete Research*. Uploaded in accordance with the publisher's self-archiving policy.

Reuse

Items deposited in White Rose Research Online are protected by copyright, with all rights reserved unless indicated otherwise. They may be downloaded and/or printed for private study, or other acts as permitted by national copyright laws. The publisher or other rights holders may allow further reproduction and re-use of the full text version. This is indicated by the licence information on the White Rose Research Online record for the item.

Takedown

If you consider content in White Rose Research Online to be in breach of UK law, please notify us by emailing eprints@whiterose.ac.uk including the URL of the record and the reason for the withdrawal request.



eprints@whiterose.ac.uk
<https://eprints.whiterose.ac.uk/>

1 **1 The Effect of Improper Curing on Properties Which May Affect Concrete**
2 **2 Durability**

3 Olusola Idowu^{1,2}, Leon Black^{1*}

4 * Corresponding author

5 ¹. School of Civil Engineering, University of Leeds, Leeds, LS2 9JT

6 ². Civil Engineering Department, Ekiti State University P.M.B. 5363, Ado -Ekiti, Ekiti
7 State, Nigeria.

8
9 **9 Abstract**

10 Good curing, enabling prolonged hydration and the development of a well-developed
11 microstructure, is imperative if concrete is to perform at its full potential. This may
12 become more important with the increasing use of composite cements containing
13 more slowly reacting additions. Furthermore, the effects of improper curing, i.e.
14 compromised durability, may not become visible for many years.

15 A series of concrete mixes have been prepared of 20 or 50 MPa target mean
16 strength, using either CEM I or CEM I + 30% fly ash as the binder. Mixes were
17 designed with two different workabilities, (10-30 and 60-180 mm slump) Samples
18 were cured in a fog room at $20 \pm 3^{\circ}\text{C}$ and $99 \pm 1\%$ RH or under ambient conditions
19 $20 \pm 3^{\circ}\text{C}$ and $42 \pm 5\%$ RH. Performance was evaluated in terms of compressive
20 strength, transport properties and resistance to carbonation. Equivalent paste
21 samples were characterised by TGA, XRD and SEM to follow hydration and
22 microstructural development.

23 Improper curing did not greatly affect compressive strength. However, the effects on
24 transport properties, and therefore properties that may affect durability, were more
25 profound. The effects of non-ideal curing were greater for lower strength mixes,
26 those containing fly ash and, to a less extent, less workable mixes.

27

28 **Keywords:** curing; durability; Permeability & pore-related properties; microstructure

29

30

31

32 **Research Significance:**

33 As society strives to reduce the carbon footprint of construction, the cement industry
34 is reducing the clinker factor by the use of additions such as fly ash. Fly ash is known
35 to hydrate more gradually than Portland cement, hence may require prolonged
36 curing. This study shows that the impact on transport properties, which may have
37 implications for durability, are more pronounced than the impact on compressive
38 strength. This study has shown that good site practice and proper curing is
39 necessary to ensure long-term concrete performance.

40

41 **1. Introduction**

42 Portland cement concrete underpins modern life. Global concrete production is
43 approaching 20×10^{12} kg per annum. Sabir *et al.* (Sabir et al., 2001) wrote that
44 concrete's consumption is second only to water as the most utilized man-made
45 substance on the planet (Meyer, 2005, Gaimster and Munn, 2007). Furthermore, as
46 vast developing nations upgrade and invest in their infrastructure, this will continue to
47 increase (Purnell and Black, 2012).

48 Portland cement is an indispensable component of concrete, but the production of
49 almost 4 billion tonnes of Portland cement per year has environmental impacts
50 (Flower and Sanjayan, 2007, Collins, 2010). The cement industry is accountable for
51 5-10 % of the anthropogenic CO₂ (Meyer, 2009, Damtoft et al., 2008, Mehta, 2001).
52 The global greenhouse gas emissions generated by production of cement has led to
53 research into how these emissions can be reduced. One such approach is the
54 increased use of supplementary cementitious materials. These materials may be in
55 their natural form, industrial by-products, or those that necessitate only minimal
56 further processing to produce. Fly ash, blast furnace slag, silica fume and metakaolin
57 are additions that can be used as partial replacements for Portland cement. These
58 materials can enhance concrete durability, lessen the risk of thermal cracking in
59 mass concrete and possess lower embodied energy- and CO₂ than Portland cement
60 (Berndt, 2009, Siddique, 2004).

61 Fly ash is an essential pozzolan, a by-product of coal combustion in the generation
62 of electricity. Most fly ash particles are spherical and amorphous, ranging in size
63 between 10 and 100 μm (Shi et al., 2012). Fly ash is an important pozzolan, and it
64 has been established that fly ash may improve the long term strength of concrete
65 with proper curing (Ramezani pour and Malhotra, 1995, Haque, 1990, Toutanji et
66 al., 2004, Thomas et al., 1989). However, fly ash hydrates more slowly than cement,
67 and thus concrete containing fly ash may require longer curing times. Curing of
68 concrete is also essential for optimal durability (Al-Gahtani, 2010), and may be
69 compromised by improper curing practices. If the concrete is not properly cured, then
70 the surface layer, about 30 to 50 mm (Neville, 2011, Gowripalan et al., 1990), is most
71 affected due to the potential for evaporation of water from the concrete surface. This
72 is particularly significant as it constitutes the cover zone for most reinforced concrete
73 construction (Gowripalan et al., 1990). This means that regulation of moisture is not

74 just for improving the compressive strength of a structure, rather it also reduces
75 surface permeability and increases hardness, so as to improve the longevity of a
76 structure, especially one exposed to harsh environments. Basheer *et.al* (Basheer et
77 al., 2001) wrote that improper curing is one of the factors that have reduced the
78 service life of many structures or resulted in mandatory comprehensive repairs, with
79 great economic costs.

80 The effects of improper curing may not appear to demonstrably affect concrete
81 quality immediately, and thus its impact on strength may not be an appropriate
82 parameter with which to measure the durability of a structure. Cabrera *et.al* (Cabrera
83 et al., 1989) commented that assessing curing methods based on the strength of the
84 concrete does not adequately predict the performance of the concrete in a structure,
85 since the durability of the concrete is controlled more by its porosity and permeability
86 than its strength.

87 One of the most important parameters influencing the durability of concrete is its
88 permeability. Permeability of concrete determines the ease with which potentially
89 deleterious substances can penetrate the concrete. Thus, permeability dictates the
90 extent to which concrete can be affected by external agents, and may thus be used
91 as a measure of concrete durability.

92 Gopalan (Gopalan, 1996) wrote that the most influential characteristics affecting
93 concrete durability were the pore structure and alkalinity of the cover concrete.
94 These factors can be followed by measuring the sorptivity and carbonation
95 resistance respectively. Furthermore, both of these factors are greatly influenced by
96 the curing conditions, with improper curing increasing permeability and reducing the
97 quantity of carbonateable matter in the hardened cement paste.

98 In addition to the use of additions to reduce the embodied carbon of concrete,
99 judicious concrete mix design can also achieve these aims (DAMINELI et al., 2013).
100 Replacement of 20% of the Portland cement in concrete can reduce the embodied
101 carbon by 14% (Black and Purnell, 2016, Purnell and Black, 2012). Meanwhile,
102 reductions in embodied carbon may be achieved by the use of a less workable
103 concrete mix. However, a truly sustainable approach should consider not just the
104 carbon footprint, but also consider long-term performance. Therefore, while stiff

105 mixes containing additions may have a lower carbon footprint, their durability must
106 also be considered.

107 This study investigates the effect of improper curing on concrete specimens. It has
108 also looked at the effect of improper curing on factors affecting durability, in
109 particular resistance to carbonation. The results have been interpreted with
110 reference to the microstructures and phase assemblages of ideally and improperly
111 cured samples.

112

113 **2. Materials and Methods**

114 **2.1 Materials**

115 Eight different concrete mixes were prepared according to the method of Teychenne
116 (Teychenné et al., 1997). The mixes were designed to examine the effects of
117 variables known to have a considerable impact on the embodied carbon of concrete
118 (Purnell and Black, 2012, Black and Purnell, 2016), namely mean compressive
119 strength, binder type and workability. The different levels of each variable are shown
120 in Table 1 and the mix designs shown in Table 2. This table also shows the
121 nomenclature used throughout the rest of this paper for naming samples.

122 Concrete specimens were cast using CEM I 52.5N, compliant with BS EN 197-1 –
123 2011 (British Standards Institution, 2011). The fly ash used complied with BS EN
124 450-1:2012 (British Standards Institution, 2012). The chemical compositions of these
125 materials, as determined by XRF, are shown in Table 3.

126
127 10 mm diameter uncrushed coarse aggregate and quartz sand of diameter 150 µm
128 to 5mm was used. Figure 1 shows the particle size distributions of the aggregates.
129 The aggregates were oven dried before use. Potable mains water within the
130 laboratory was used.

131 Concrete specimens were prepared for compressive strength, permeability, sorptivity
132 and carbonation testing. Samples were cast in steel moulds and covered with
133 polythene sheeting. After 24 hours samples were stripped from the moulds and
134 cured under one of two conditions; one in the fog room at temperature of 20 ± 3 °C
135 and $99 \pm 1\%$ RH and the second one under ambient conditions at 20 ± 3 °C, $42 \pm 5\%$

136 RH. These curing conditions are henceforth referred to as ideal and ambient
137 respectively.

138

139 **2.2 Methods**

140 **2.2.1 Compressive strength test**

141 The compressive strength of 100 X 100 X 100 mm concrete cubes was determined
142 in triplicate after curing for 28 days. The unconfined compressive strength was
143 measured using a Retrofit Tonipact Concrete and Transverse Beam Machine
144 according to BS EN 12390-3 (British Standards Institution, 2009). The ideally-cured
145 samples were tested immediately after removal from the fog room, the cubes just
146 being made surface dry with a towel before testing. The samples cured under
147 ambient conditions however were immersed in water for 3 hours prior to testing. This
148 was to remove any influence of the degree of sample saturation on the measured
149 strength (Chen et al., 2012, Shoukry et al., 2011).

150 **2.2.2 Permeability test**

151 Concrete permeability was measured by using a gas permeability cell developed by
152 Cabrera and Lynsdale (Cabrera and Lynsdale, 1988). Figure 2 shows the
153 Components of the Leeds cell used for the permeability test. Concrete samples of
154 50mm diameter and 40mm height were cast and cured for 28 days. Following curing,
155 the samples were placed in an oven to dry to constant weight at $40 \pm 2^\circ\text{C}$. This
156 drying temperature was selected as being high enough to allow for pore water to be
157 driven off in a reasonable time and not so high as to result in decomposition of the C-
158 S-H or the ettringite. Concrete samples (S) were placed into the rubber cylinder (A)
159 which was placed into the plastic ring cylinder (B). This was placed into the Leeds
160 cell and the metal O ring (C) was put in place before the cell cap (D) was positioned.
161 A force was applied vertically downward to form a seal to ensure that all nitrogen
162 passing through the system would go directly through the sample.

163

164 Nitrogen gas was forced through the sample at a defined pressure after which the
165 flow was allowed to normalise to a steady flow (generally 10-15 minutes). The time
166 for a known volume of nitrogen to pass through the sample was recorded by using a

167 bubble flow meter. This was repeated three times to provide an average and
168 standard deviation and to ensure that the flow had fully normalised.

169 This procedure was repeated for each sample at different applied pressures; 0.5,1,
170 1.5,2 and 2.5 bar (above atmospheric). Ten millimetres (10mm) flowmeter tube was
171 used for more permeable samples, and five millimetres (5mm) for less permeable
172 samples. All mixes were tested in triplicate at 28 days following curing under
173 standard and ambient conditions.

174 Permeability was then calculated according to the method proposed by Grube and
175 Lawrence (Grube and Lawrence, 1984), with a slight alteration to take account for
176 the change in gas, as shown in equation below.

$$k = \frac{2P_2 \times vL \times 1.78 \times 10^{-6}}{A(P_1^2 - P_2^2)}$$

178 Where: P_1 is the absolute applied pressure (bar), P_2 is pressure at which the flow
179 rate is measured in bar and is 1.01325 bar, v is measured in cm^3/s , L and a
180 measured in m and 1.78×10^{-6} = dynamic viscosity of nitrogen at 20°C (g/cm/s).

2.2.3 Sorptivity tests

182 Sorptivity tests were carried out using similar methods by Tasdemir (Tasdemir, 2003)
183 and Güneyesi (Güneyesi and Gesoğlu, 2008), on concrete cubes which had been
184 cured for 28 days and dried in an oven at 40°C to constant mass. A schematic
185 diagram showing the set-up of the sorptivity test is presented in Figure 3. After
186 drying, the lower areas on the sides of the specimens were coated with petroleum
187 jelly so as to ensure unidirectional flow; the coated samples were placed in a trough
188 of water, with the water level kept at about 5mm from the base of the specimens.
189 The specimens were removed from the trough and weighed at different time intervals
190 up to one hour to evaluate mass gain. At each of these times, the mass of water
191 adsorbed by each of the specimen was obtained, and from this the sorptivity
192 coefficient (k) was calculated according to

$$K = \frac{Q}{A\sqrt{t}}$$

195 Where Q is the amount of water adsorbed in m^3 , t is the time in secs, A is the cross-
196 sectional area of the specimen that was in contact with the water in m^2 , and k is the
197 sorptivity coefficient in $m^3/m^2s^{1/2}$.

199 **2.2.4 Carbonation**

200 The depth of carbonation was determined on cubes cured for 28 days. After curing,
201 samples were allowed to dry in an ambient environment for two weeks, as stated in
202 clause 6.2.7 of BS 1881 – 210(British Standards Institution, 2013). This step is
203 necessary to stabilize the internal relative humidity of the concretes, and reduce the
204 variation in the internal relative humidity between the concrete samples before
205 subjecting them to accelerated carbonation tests. Samples were then exposed to
206 pure CO_2 for two weeks at $20^\circ C$ and 65% RH (using a saturated NaBr solution).
207 Carbonation depths were determined by spraying a freshly broken surface with
208 alcoholic 1% phenolphthalein solution. The average depths of carbonation were
209 measured at two points perpendicular to three faces of the broken concrete cubes.
210 The depths of penetration of the trowelled face were ignored due to the influence of
211 trowelling.

213 **2.3 Sample preparation for SEM, XRD and TG Samples**

214 Paste samples were used for SEM, XRD and TG analysis, as the presence of quartz
215 in concrete samples can affect the accuracy of the tests. Samples were prepared by
216 using the same water / binder ratio as used for the concrete mixes. The fresh
217 prepared pastes were poured into 14-16mm diameter, 8 ml plastic tubes, fitted with
218 tight lids and placed in tube rotator at ten rph overnight to prevent any bleeding and
219 segregation. The samples were removed from the rotator after 12 hours, whereupon
220 the ideally cured samples were sealed and cured in a water bath at $23^\circ C$, while the
221 plastic tubes for the ambient-cured samples were left open at both ends, and left to
222 cure under ambient conditions. The samples were cured for 1, 7 and 28 days. The
223 cured samples were cut using an isomet slow speed saw. After removal of the outer
224 1mm, two 2 mm thick slices were cut from each end and hydration stopped by
225 solvent exchange. The four slices were immersed in isopropyl alcohol (IPA)
226 overnight using a solution-to-sample ratio of 100:1 followed by drying in a vacuum

227 desiccator for another 12 hours. The outermost of these 2 mm slices was used for
228 SEM imaging, imaging the surface 3 mm from the end of each tube.

230 2.3.1 XRD

231 Hydration stopped paste samples from the second slice, i.e. 3-5mm into the sample,
232 were ground to a fine powder with a pestle and mortar before being placed in a
233 10mm diameter holder using the back loading method. In order to minimise the effect
234 of preferred orientation, samples were prepared carefully and minimal pressure was
235 applied when back loading the samples onto the sample holders (Aranda et al.,
236 2012). A Bruker D2 Phaser with a Cu X-ray source working at 300W (30KV at 10mA)
237 was used. The scan step size was 0.02°, the collection time 1s, and patterns were
238 collected over the range 7° to 70° 2θ with effective total time of 3403 s. The
239 divergence slit, air scatter, filter and Soller slits were set to 1, 1, 0.5 and 2.5
240 respectively.

242 2.3.2 TGA

243 Powder samples prepared as for XRD analysis were also used for thermal analysis.
244 The portlandite (CH) and bound water W_n contents were measured by thermal
245 gravimetric analysis (TGA). A Stanton Redcroft Thermal Gravimetric Analyser TG
246 760 was used. Samples of ≈ 6-8mg were loaded in a clean crucible and heated
247 under nitrogen from 20° to 1000°C at a constant rate of 20°C/min. The tangent
248 method was used to evaluate the portlandite (CH) content and the equivalent (CH)_{eq}
249 from the calcium carbonate (CaCO₃) content. The sum of the CH and (CH)_{eq}
250 contents were used to assess the degree of hydration of each sample. The following
251 equations were used to calculate the CH

$$252 \quad \%Ca(OH)_2 = \left(ML_{CH} \times \frac{M_{CH}}{M_{H_2O}} \right) \div \text{Residue}$$

$$254 \quad CaCO_3 = \left(ML_{CaCO_3} \times \frac{M_{CaCO_3}}{M_{CO_2}} \right) \div \text{Residue}$$

$$255 \quad [Ca(OH)_2]_{eq} = \left(ML_{CaCO_3} \times \frac{M_{Ca(OH)_2}}{M_{CO_2}} \right)$$

256 Where:

257 ML_{CH} mass loss due to dehydroxylation of CH

258 ML_{CaCO_3} mass loss due to decarbonation of $CaCO_3$

259 M_{CH} molar mass of CH, taken as 74g/ mol

260 M_{H_2O} molar mass of water, taken as 18g/mol

261 M_{CaCO_3} molar mass of $CaCO_3$. $M_{CaCO_3} = 100g/mol$

262 M_{CO_2} molar mass of $CO_2 = 44g/mol$

263 Total CH = $\%Ca(OH)_2 + [Ca(OH)_2]_{eq}$

264

265 The bound water was taken as the mass loss between 50 °C and 550 °C, at which
266 point it was assumed that all the phases containing water had fully decomposed. W_n ,
267 normalised to the total mass loss at 550°C was calculated using the equation as
268 described by Whittaker *et al.* (Whittaker et al., 2014).

$$269 \quad W_n = \left(\frac{W_{50} - W_{550}}{W_{550}} \right) \times 100$$

270 Where:

271 W_{550} mass loss at 550°C

272 W_{50} mass loss at 50°C

273

274

275

276 2.3.3 SEM

277 SEM samples were prepared from ambient and ideal cured samples which had been
278 cured for 28 days. The 2mm thick sample which had been cut and hydration stopped
279 was resin impregnated and polished using silicon carbide paper and then diamond
280 paste. The sample was placed in the resin such that the cut surface was to be
281 viewed. As such, the degree of hydration was measured at a depth of 1mm from the
282 surface of the paste. A Jeol 5900 LV scanning electron microscope fitted with a
283 backscatter electron detector was used for imaging. An accelerating voltage of
284 15KeV and 10mm working distance was used. The degree of hydration was
285 measured on 25 images obtained at 400X magnification using the method described
286 by Whittaker(Whittaker et al., 2014).

287 A consistent analysis technique was applied to all the images by using a grey level
 288 histogram as shown in below Figure 4. The histogram was obtained for each image.
 289 Four components of the hydrated paste microstructure: capillary porosity, calcium
 290 hydroxide (CH), calcium silicate hydrate gel along with other hydration products, and
 291 unhydrated cement could be identified in the histogram. The histogram also indicates
 292 the number of pixels in the image having each possible brightness value (between 0
 293 and 225). Pores in the microstructure appear as dark spots on the electron images
 294 and can be easily distinguished from the hydrated phases (C-S-H and CH), C-S-H
 295 are dark grey

296
 297 The Java applet Image J was used to calculate the amount of unreacted cement,
 298 from which the equation below was used to calculate the degree of hydration for
 299 cement and fly ash blends.

300
 301
$$DH_{SEM}^{cem}(t) = 1 - \frac{V_{(t)cem}}{V_{(o)cem}}$$

302
 303
$$DR_{SEM}^{Add}(t) = 1 - \frac{V_{(t)Add}}{V_{(o)Add}}$$

304
 305 Where:

- 306 $V_{(o)cem}$ is the volume fraction of cement before hydration
 307 $V_{(o)Add}$ is the volume fraction of unreacted addition before hydration
 308 $V_{(t)cem}$ is the volume fraction of unhydrated cement at hydration time t, and
 309 $V_{(t)Add}$ is the volume fraction of unreacted addition at hydration time t.

310
 311 **3. Results**

312 **3.1 Compressive strength**

313 The 28 day compressive strengths of ambient- and ideal-cured CEM I and fly ash
 314 blend concretes is presented in Figure 5. In all instances the ideal-cured samples
 315 had higher strengths than the ambient-cured samples, in agreement with other
 316 findings (Xue et al., 2015, Ozer and Ozkul, 2004, Nahata et al., 2014). This effect
 317 was more pronounced for the lower strength samples. While it is known that samples

318 exposed to ambient conditions should develop lower strengths due to reduced
319 degrees of hydration, it is assumed that the effect of improper curing diminishes with
320 increasing compressive strength because the lower water/binder ratios inhibit water
321 loss under ambient conditions. This was supported by the reduced permeability and
322 sorptivity results for the higher strength samples (see below).

323 Comparing the results from the CEM I and fly ash blends, ambient curing appeared
324 to have a slightly more detrimental effect on the composite cement mixes. Similar
325 results were obtained by other researches (Ramezaniapour and Malhotra, 1995,
326 Cao et al., 2000, Ozer and Ozkul, 2004, Tan and Gjør, 1996, Nassif and
327 Suksawang, 2002, Güneyisi et al., 2005, Aprianti et al., 2016) .This is perhaps as
328 expected, since drying of the samples under ambient conditions is not
329 instantaneous, thus the CEM I concretes will have hydrated to a greater degree than
330 the blended cement systems, binding water and thus not allowing it to evaporate.
331 Running counter to this, however, the increased rate of early-age clinker hydration
332 when fly ash was present (see later), due to the filler effect and higher effective
333 water/cement ratio, may have made the loss of performance less than may have
334 been expected.

335

336 3.2 Sorptivity

337 Figure 6 shows the sorptivity data from the various samples. The sorptivity
338 coefficients of ambient-cured concretes were considerably higher than those of the
339 ideal-cured samples. This is in agreement with the findings of Khatib and Mangat
340 who found that trowelled faces of concrete cubes cured to ambient conditions
341 showed higher sorptivity and water absorption values than the centre of their cubes.
342 It also agrees with the findings of others (Tasdemir, 2003, Bai et al., 2002, Khatib
343 and Mangat, 1995). The figure also shows that sorptivity decreased with increasing
344 compressive strength, and that non-ideal curing had a greater effect on the lower
345 strength mixes.

346 Wet mixes often showed higher sorptivities than the corresponding stiff mixes, and
347 non-ideal curing also seemed to have a slightly greater effect on the wet mixes than
348 the corresponding stiff mixes, but the effect was not too clear cut. The increased

349 paste volume in the wet mixes may be the cause of this slightly elevated
350 permeability.

351 Finally, the importance of ideal curing conditions for composite cements is clear in
352 the figure. For the ideally cured samples, the fly ash-containing blends normally had
353 lower sorptivities than their corresponding CEM I blends (Nath and Sarker, 2011,
354 Camões et al., 2003, Gopalan, 1996, Khan and Lynsdale, 2002, Kelham, 1988, Bai
355 et al., 2002). However, under ambient curing conditions, the situation was reversed
356 and the fly ash blends all showed worse performance than the equivalent CEM I
357 concretes. Again, similar findings were seen by Khatib and Mangat as a function of
358 depth from the trowelled face of ambient-cured concrete specimens.

360 **3.3 Permeability**

361 The permeability results from the various samples are presented in Table 4. For the
362 ideally cured samples, permeability decreased with increasing strength, as would be
363 expected. Workability also had an effect on permeability, with stiff mixes generally
364 having lower permeabilities than their corresponding wet mixes. The effect of binder
365 type was less clear-cut. Stiff fly ash-containing concretes had higher permeabilities
366 than their CEM I equivalents, but wet fly ash-containing mixes showed lower
367 permeabilities.

368 The impact of improper curing on all samples was immediately clear, there being at
369 least a ten-fold increase in permeability for almost all ambient-cured samples
370 compared to their ideal-cured equivalents. The key factor in determining the effect of
371 improper curing on permeability was the compressive strength, with the 20 MPa
372 samples exhibiting an average increase in permeability about 50% greater than the
373 50 MPa samples. While wet mixes generally showed higher permeabilities than their
374 equivalent stiff mixes, both following ideal and ambient curing, concrete workability
375 did not appear to influence the extent of the increase in permeability upon ambient
376 curing. Somewhat surprisingly, binder type did not appear to have a clear effect on
377 permeability but addition of fly ash reduces the permeability which can be seen in the
378 table that permeability of ideal cured fly ash samples having lower permeability than
379 CEM1 samples and this is in agreement with other researchers (Beglarigale et al.,
380 2014, Dhir et al., 1987, Khan and Lynsdale, 2002).

381

382 **3.4 Resistance to carbonation**

383 Figure 7 shows the carbonation depth measured for the 20 MPa samples. Ambient
384 curing had a detrimental effect on carbonation resistance. The improvement in
385 carbonation resistance with improved curing conditions has been shown previously
386 (Das et al., 2011, Atiş, 2003, Ewertson and Petersson, 1993, Roziere et al., 2009, Lo
387 and Lee, 2002, Balayssac et al., 1995, Fattuhi, 1988, Younsi et al., 2013). Stiff mixes
388 showed slightly higher carbonation rates than wet mixes, but the impact of improper
389 curing was not related to concrete workability. Similar conclusions could be made
390 concerning binder type, where there were no clear, consistent trends in the data but
391 ideally cured fly ash blends performed better than the equivalent CEM I mixes (Das
392 and Pandey, 2011, Das et al., 2011, Atiş, 2003). This is in line with the permeability
393 data.

394

395 **3.5 Degree of hydration**

396 In the previous sections, it has been demonstrated that non-ideal curing affected
397 strength development and transport properties. The loss of water from the hydrating
398 cement, prior to complete hydration, had impaired performance. As discussed, the
399 presence of water is essential for continued hydration. Therefore, paste samples
400 were prepared with matching water/binder ratios to equivalent concrete samples and
401 cured under ideal or non-ideal conditions. These paste samples were then
402 characterised to determine the degree of cement hydration, which could then be
403 related to the engineering performance measures detailed above.

404 Figures 8 and 9 show selected SEM images of ambient and ideal cured samples of
405 CEM I and fly ash paste. The field of view in each image is 326 x 244 μm . The
406 samples show a mixture of hydrated cement paste, residual anhydrous material and
407 coarse porosity (with the smallest feature being ca. 2x2 microns) (Whittaker et al.,
408 2014). The figures therefore allow an assessment of the degree of cement hydration
409 and of coarse capillary porosity.

410 The figures show how, as expected, capillary porosity was greater for the lower
411 strength samples. The wet mixes were more porous than the equivalent dry mixes.
412 This is in line with the intrinsic permeability measurements presented earlier.

1 413 Meanwhile, changing the binder from CEM I to a fly ash blend did not appear to have
2 414 a significant effect on the microstructure.

3
4 415 Most clearly, ambient-cured samples exhibited reduced degrees of hydration,
5
6 416 evidenced by the increased presence of anhydrous clinker (appearing as bright
7
8 417 angular features), and much higher capillary porosities than their ideal-cured
9
10 418 counterparts. The figures are a clear indication of how ideal curing can improve the
11
12 419 pore structure of concrete, as has been reported by others previously (Mangat and
13
14 420 El-Khatib, 1992, Khatib and Mangat, 1999, El-Sakhawy et al., 1999, Toutanji et al.,
15
16 421 2004, Elahi et al., 2010).

17 422 Using the approach developed elsewhere (Kocaba, 2009, Whittaker et al., 2014),
18
19 423 and as described in 2.3.3, it was then possible to determine the degree of clinker
20
21 424 hydration in each of the samples. Table 5 and Figure 10 show the degree of clinker
22
23 425 hydration for each of the samples. In all cases, the ideal cured samples showed a
24
25 426 higher degree of hydration than their corresponding ambient cured ones, confirming
26
27 427 that prolonged moist hydration increases the degree of hydration (Bentz et al., 1997,
28
29 428 Chen and Wu, 2013). Allowing the samples to dry under ambient curing conditions
30
31 429 affected hydration, in turn leading to higher porosity and coarser pore structure
32
33 430 compared to ideal-cured concrete (Patel et al., 1988).

34 431 Workability had no discernible effect on the degree of hydration.

35
36 432
37
38 433 Figure 10 also shows that the degree of clinker hydration was consistently higher for
39
40 434 the fly ash-containing blends than their corresponding CEM I samples, irrespective of
41
42 435 curing conditions. This may be ascribed to the filler effect and increased effective
43
44 436 water/cement ratio at early ages (Lawrence et al., 2003, Hanehara et al., 2001, Pane
45
46 437 and Hansen, 2005, Lam et al., 2000, Sakai et al., 2005). Note also that, while the
47
48 438 degree of clinker hydration is higher, this doesn't necessarily relate to the overall
49
50 439 degree of binder hydration because the fly ash will only have reacted to a small
51
52 440 degree (Poon et al., 2000, Lam et al., 2000, Li et al., 2000).

53 441

54
55
56 442 **3.6 Bound water content**

57
58 443 The hydration of cementitious materials can be examined by the bound water
59
60 444 content. Bound water content cannot be directly related to the overall degree of

445 hydration but gives an indication of the progress of hydration (Whittaker et al., 2014,
446 Pane and Hansen, 2005). Figure 11 shows the bound water content calculated for
447 each sample at 28 days. As expected, the bound water contents of the ideal cured
448 samples were higher than those of the ambient cured samples. This is a reflection of
449 the higher degree of hydration, as evidenced by the SEM data and supporting the
450 improved engineering performance.

451 As with many of the other measures, the workability of the sample did not appear to
452 have an effect on the bound water content. The binder type, however, did affect the
453 bound water content. All of the fly ash-containing samples showed lower bound
454 water contents than the corresponding CEM I mixes. This is due to the low reactivity
455 of the fly ash compared to the cement clinker and explains why, despite the higher
456 degree of clinker hydration (as determined by SEM-BSE analysis) the engineering
457 performance of the fly ash-containing concretes was not significantly better than that
458 of the corresponding CEM I concretes. Furthermore, comparing the difference in
459 bound water content for ideal and ambient cured samples according to binder type,
460 the presence of fly ash in the concrete did not appear to affect the susceptibility to
461 improper curing.

3.7 Thermogravimetry

464 Tables 6 and 7 show the CH content calculated from thermogravimetric analysis
465 (TGA) of all the samples. Note that, since CH is a hydration product of cement, the
466 CH content of the fly ash blends had been normalised to cement content (by dividing
467 the obtained data by 0.7) in order to compare the results with the CEM I results.

468 For the CEM I systems, the portlandite contents were always higher when the
469 samples were cured under ideal conditions, i.e. hydration had been allowed to
470 proceed, so had led to the formation of portlandite from the hydration of alite and
471 belite. However, the situation for the fly ash-containing samples was different. In
472 these samples, the ideally cured specimens invariably had lower portlandite
473 contents. This is due to the consumption of portlandite during the pozzolanic
474 reaction.

3.8 XRD

477 Qualitative XRD analysis was carried out to examine the effect of curing on the
478 hydration of the clinker phases present in the mixes. Figures 12 and 13 show typical
479 XRD patterns obtained from CEM I and fly ash-containing pastes obtained after
480 hydration for 1, 7 and 28 days. The reflections for portlandite (at 18° , 34° and $47^\circ 2\theta$)
481 can be considered as a good indicator of the evolution of hydration reactions
482 (Mounanga et al., 2004, WANG et al., 2005). Ideal curing led to increased portlandite
483 contents in the CEM I samples, while the portlandite contents in the ambient-cured
484 samples did not increase so dramatically. Similarly, the decrease in the intensity of
485 the peaks due to alite and belite, (near $29.5^\circ 2\theta$) was more profound under ideal
486 curing conditions.

487 As with the thermogravimetric data, the production of portlandite under ideal curing
488 conditions was not so pronounced in the fly ash-containing mixes. The pozzolanic
489 reaction led to portlandite consumption when the samples were cured under ideal
490 conditions. However, the aforementioned consumption of alite and belite could be
491 observed.

492

493 **Conclusions**

494 The study shows that improper curing is detrimental to the performance of concrete.
495 Improper curing leads to reduced compressive strength development and increased
496 sorptivity and permeability. This is due to reduced levels of cement hydration as
497 water evaporates from the concrete surface. This study has shown that the impact
498 on sorptivity and permeability is far greater than the impact on compressive strength,
499 with implications for the long-term durability of concrete.

500 The extent of the impact of improper curing depends on the properties of the
501 concrete. Low strength concrete, which has a slightly higher water content and also
502 an inherently higher porosity, is more greatly affected by improper curing than high
503 strength concrete. This is presumed to be due to the ease with which water can
504 evaporate from the surface of the more porous cement paste.

505 Composite cements, containing 30% fly ash, showed comparable strengths to CEM I
506 concretes and improved transport properties when ideally cured. Improper curing
507 however led to reduced performance. Strength was compromised by improper curing
508 to a greater degree than for equivalent CEM I mixes. However, it was sorptivity and

1 509 permeability which were most severely affected. This was due to the reduced degree
2 510 of cement hydration which will have affected the pozzolanic reaction between the fly
3 ash and portlandite.
4 511
5
6 512 Concrete workability has been found to be a factor which can help to reduce the
7 embodied carbon of concrete (Purnell & Black, 2012), with stiffer mixes having lower
8 513 carbon footprints. This study has shown that while stiff concrete mixes may show
9 514 improved transport properties, their lower paste volumes leave them more
10 515 susceptible to carbonation.
11
12 516
13
14 517 This study confirms the need for good site practice, and also shows that embodied
15 carbon should not be the only factor when considering the environmental
16 518 performance of concrete. Rather, durability and whole life performance should also
17 519 be considered.
18
19 520
20
21 521
22
23
24
25
26
27
28
29
30
31
32
33
34
35
36
37
38
39
40
41
42
43
44
45
46
47
48
49
50
51
52
53
54
55
56
57
58
59
60
61
62
63
64
65

522 Table 1 Variables used in the mix design

Variable	Level
UCS	20 MPa 50 MPa
Workability (slump)	10-30 mm (stiff) 60-180 mm (wet)
Binder	CEM I 52.5N 70 % CEM I 52.5N + 30% fly ash

523

524 Table 2: Mix designs used for the samples in this study. Note, water contents were
525 those used having accounted for moisture uptake by the oven dried aggregates.

Binder type	Target strength (MPa)	Slump (mm)	Nomenclature	W/b ratio	Water (kg/m ³)	Cement (kg/m ³)	PFA (kg/m ³)	Fine aggregate (kg/m ³)	Coarse aggregate (kg/m ³)
CEM1	20	10-30	20 S-C	0.77	212.9	275	0	849	1033
	50		50 S-C	0.42	207.4	499	0	650	1007
CEM1	20	60-180	20 W-C	0.75	257.2	343	0	911	805
	50		50 W-C	0.40	250.5	624	0	675	760
30% fly ash	20	10-30	20 S-FA	0.78	197.7	223	96	844	1026
	50		50 S-FA	0.42	191.6	405	174	631	978
30% fly ash	20	60-180	20 W-FA	0.76	237.0	277	119	906	801
	50		50 W-FA	0.40	229.6	504	216	651	732

526

527 Table 3 Compositions of raw material, determined by XRF (% weight)

Compound	%	CEM I	Fly ash
SiO ₂	%	19.85	50.73
Al ₂ O ₃	%	4.93	25.49
Fe ₂ O ₃	%	2.14	10.05
CaO	%	63.95	2.28
MgO	%	2.01	1.63
SO ₃	%	3.13	0.41
K ₂ O	%	0.58	3.46
Na ₂ O	%	0.37	0.90

528

529

530

531 Table 4 Ambient and Ideal Permeability coefficients.

	Ideal cured (10^{-16} m^2)	Ambient cured (10^{-16} m^2)	Percentage increase upon ambient curing
20MPa Stiff mix CEM I	0.29	6.26	2160
50MPa Stiff mix CEM I	0.14	1.65	1180
20MPa Wet mix CEM I	0.61	7.00	1150
50MPa Wet mix CEM I	0.23	2.01	870
20MPa Stiff mix fly ash	0.45	6.38	1420
50MPa Stiff mix fly ash	0.16	1.64	1030
20MPa Wet mix fly ash	0.30	5.60	1870
50MPa Wet Mix fly ash	0.21	2.57	1220

532

533 Table 5 Degree of hydration obtained from SEM Images

	Ambient DOH	Ideal DOH
20 Stiff mix CEM1	79.58	82.81
50 Stiff mix CEM1	60.9	73.68
20 Wet mix CEM1	73.08	81.76
50 Wet mix CEM1	66.22	73.02
20 Stiff mix fly ash	86.83	91.55
50 Stiff mix fly ash	80.87	87.62
20 Wet mix fly ash	81.13	92.15
50 Wet mix fly ash	81.63	90.61

534

535

536 Table 6: Portlandite contents determined by thermal analysis for each CEM I mix

Mix	Age	Ca(OH) ₂	CaCO ₃	Ca(OH) _{2eq}	CH total
20MPa Stiff mix	Ambient	6.52	5.41	3.03	9.55
20MPa Stiff mix	Ideal	9.74	0.90	0.50	10.24
50MPa Stiff mix	Ambient	6.91	2.26	1.35	8.26
50MPa Stiff mix	Ideal	8.42	0.00	0.00	8.42
20MPa Wet Mix	Ambient	7.51	3.56	2.02	9.53
20MPa Wet Mix	Ideal	10.37	2.72	1.51	11.89
50MPa Wet mix	Ambient	7.29	2.59	1.51	8.80
50MPa Wet Mix	Ideal	7.37	1.02	0.59	7.96

537

538 Table 7: Portlandite contents determined by thermal analysis for each fly ash-
539 containing mix (note data have been normalised to cement content).

Mix	Age	Ca(OH) ₂	CaCO ₃	Ca(OH) _{2eq}	CH total
20MPa Stiff mix	Ambient	8.06	2.51	1.51	9.57
20MPa Stiff mix	Ideal	8.21	1.98	1.18	9.38
50MPa Stiff mix	Ambient	7.43	5.21	3.20	10.63
50MPa Stiff mix	Ideal	7.05	1.95	1.18	8.23
20MPa Wet Mix	Ambient	6.04	4.73	2.86	8.90
20MPa Wet Mix	Ideal	8.04	1.86	1.09	9.14
50MPa Wet Mix	Ambient	6.43	4.10	2.52	8.96
50MPa Wet Mix	Ideal	7.18	1.84	1.09	8.28

540

541

542

1
2
3
4
5
6
7
8
9
10
11
12
13
14
15
16
17
18
19
20
21
22
23
24
25
26
27
28
29
30
31
32
33
34
35
36
37
38
39
40
41
42
43
44
45
46
47
48
49
50
51
52
53
54
55
56
57
58
59
60
61
62
63
64
65

List of Figure Captions

- 544 Figure 1 Aggregate grading curves
- 545 Figure 2: Components of the Leeds cell
- 546 Figure 3 Schematic setup of sorptivity test
- 547 Figure 4: Grey level histogram of a hydrated cement paste
(AN: the unreacted cement, CH: calcium hydroxide, C-S-H: calcium silicate hydrate
548 gel along with other hydration products, Capillary porosity)
- 549
- 550 Figure 5: Mean unconfined compressive strengths of ambient- and ideal-cured
551 concretes at 28 days. (The percentages represent the average strength loss due to
552 ambient curing)
- 553 Figure 6: Sorptivity of ambient- and ideal-cured CEM I and fly ash-bearing concretes
- 554 Figure 7 Carbonation depth of ambient and ideal cured CEM I and fly ash concrete
- 555 Figure 8: SEM images of CEM I stiff mixes cured under ambient and ideal
556 conditions.
- 557 Figure 9 SEM images of fly ash-containing wet mixes cured under ambient and ideal
558 conditions.
- 559 Figure 10: Degree of hydration of ambient and ideal cured samples measured from
560 BSE images
- 561 Figure 11: Bound water content of ambient and ideal cured samples
- 562 Figure 12 XRD patterns obtained from CEM I pastes with a w/c ratio of 0.6, i.e. the
563 same as the 20MPa stiff mix, cured under ideal or ambient conditions for up to 28
564 days. (CH indicates portlandite and * indicates the cluster of reflections attributed to
565 a mixture of alite and belite)
- 566 Figure 13 XRD of 20MPa fly ash stiff mix from 1 day to 28days of curing

569 **List of Table Captions**

1
2
3
4
5
6
7
8
9
10
11
12
13
14
15
16
17
18
19
20
21
22
23
24
25
26
27
28
29
30
31
32
33
34
35
36
37
38
39
40
41
42
43
44
45
46
47
48
49
50
51
52
53
54
55
56
57
58
59
60
61
62
63
64
65

570 Table 1 Variables used in the mix design

571 Table 2: Mix designs used for the samples in this study. Note, water contents were
572 those used having accounted for moisture uptake by the oven dried aggregates.

573 Table 3 Compositions of raw material, determined by XRF (% weight)

574 Table 4 Ambient and Ideal Permeability coefficients.

575 Table 5 Degree of hydration obtained from SEM Images

576 Table 6: Portlandite contents determined by thermal analysis for each CEM I mix

577 Table 7: Portlandite contents determined by thermal analysis for each fly ash-
578 containing mix (note data have been normalised to cement content).

579

580

- 581 AL-GAHTANI, A. 2010. Effect of curing methods on the properties of plain and
1 582 blended cement concretes. *Construction and Building Materials*, 24, 308-314.
2
- 3 583 APRIANTI, E., SHAFIGH, P., ZAWAWI, R. & HASSAN, Z. F. A. 2016. Introducing an
4 584 effective curing method for mortar containing high volume cementitious
5 585 materials. *Construction and Building Materials*, 107, 365-377.
6
- 7 586 ARANDA, M. A., ÁNGELES, G. & LEÓN-REINA, L. 2012. Rietveld quantitative
8 587 phase analysis of OPC clinkers, cements and hydration products. *Reviews in
9 588 Mineralogy and Geochemistry*, 74, 169-209.
10
- 11 589 ATIŞ, C. D. 2003. Accelerated carbonation and testing of concrete made with fly ash.
12 590 *Construction and Building Materials*, 17, 147-152.
13
- 14 591 BAI, J., WILD, S. & SABIR, B. 2002. Sorptivity and strength of air-cured and water-
15 592 cured PC–PFA–MK concrete and the influence of binder composition on
16 593 carbonation depth. *Cement and Concrete Research*, 32, 1813-1821.
17
- 18 594 BALAYSSAC, J., DÉTRICHÉ, C. H. & GRANDET, J. 1995. Effects of curing upon
19 595 carbonation of concrete. *Construction and Building Materials*, 9, 91-95.
20
- 21 596 BASHEER, L., KROPP, J. & CLELAND, D. J. 2001. Assessment of the durability of
22 597 concrete from its permeation properties: a review. *Construction and building
23 598 materials*, 15, 93-103.
24
- 25 599 BEGLARIGALE, A., GHAJERI, F., YIĞİTER, H. & YAZIÇI, H. 2014. Permeability
26 600 Characterization of Concrete Incorporating Fly Ash.
27
- 28 601 BENTZ, D. P., SNYDER, K. A. & STUTZMAN, P. E. Hydration of Portland cement:
29 602 The effects of curing conditions. Proceedings of the 10th International
30 603 Congress on the Chemistry of Cement, 1997.
31
- 32 604 BERNDT, M. 2009. Properties of sustainable concrete containing fly ash, slag and
33 605 recycled concrete aggregate. *Construction and Building Materials*, 23, 2606-
34 606 2613.
35
- 36 607 BERODIER, E. M. J. 2015. *Impact of the supplementary cementitious materials on
38 608 the kinetics and microstructural development of cement hydration*. ÉCOLE
39 609 POLYTECHNIQUE FÉDÉRALE DE LAUSANNE.
40
- 41 610 BLACK, L. & PURNELL, P. 2016. Is carbon dioxide pricing a driver in concrete mix
42 611 design? *Magazine of Concrete Research*, 68, 561-567.
43
- 44 612 BRITISH STANDARDS INSTITUTION 2009. BS EN 12390-3 Testing hardened
45 613 concrete Part 3: Compressive strength of test specimens.
46
- 47 614 BRITISH STANDARDS INSTITUTION 2011. BS EN 197-1 Cement Part 1:
48 615 Composition, specifications and conformity criteria for common cements.
49
- 50 616 BRITISH STANDARDS INSTITUTION 2012. BS EN 450-1 Fly ash for concrete Part
51 617 1: Definition, specifications and conformity criteria.
52
- 53 618 BRITISH STANDARDS INSTITUTION 2013. BS 1881-210:2013: Testing hardened
54 619 concrete. Determination of the potential carbonation resistance of concrete.
55 620 Accelerated carbonation method.
56
- 57 621 CABRERA, J., GOWRIPALAN, N. & WAINWRIGHT, P. 1989. An assessment of
58 622 concrete curing efficiency using gas permeability. *Magazine of Concrete
59 623 Research*, 41, 193-198.
60

- 624 CABRERA, J. & LYNSDALE, C. 1988. A new gas permeameter for measuring the
1 625 permeability of mortar and concrete. *Magazine of Concrete Research*, 40,
2 626 177-182.
3
- 4 627 CAMÕES, A., AGUIAR, J. & JALALI, S. 2003. Durability of low cost high
5 628 performance fly ash concrete.
6
- 7 629 CAO, C., SUN, W. & QIN, H. 2000. The analysis on strength and fly ash effect of
8 630 roller-compacted concrete with high volume fly ash. *Cement and concrete
9 631 research*, 30, 71-75.
10
- 11 632 CHEN, X., HUANG, W. & ZHOU, J. 2012. Effect of moisture content on compressive
12 633 and split tensile strength of concrete. *Indian Journal of Engineering &
13 634 Materials Sciences*, 19, 427-435.
14
- 15 635 CHEN, X. & WU, S. 2013. Influence of water-to-cement ratio and curing period on
16 636 pore structure of cement mortar. *Construction and Building Materials*, 38, 804-
17 637 812.
18
- 19 638 COLLINS, F. 2010. Inclusion of carbonation during the life cycle of built and recycled
20 639 concrete: influence on their carbon footprint. *The International Journal of Life
21 640 Cycle Assessment*, 15, 549-556.
22
- 23 641 DAMINELI, B., PILEGGI, R. & JOHN, V. 2013. Lower binder intensity eco-efficient
24 642 concretes. *Eco-efficient concrete*, 1.
25
- 26 643 DAMTOFT, J., LUKASIK, J., HERFORT, D., SORRENTINO, D. & GARTNER, E.
27 644 2008. Sustainable development and climate change initiatives. *Cement and
28 645 concrete research*, 38, 115-127.
29
- 30 646 DAS, B., SINGH, D. & PANDEY, S. 2011. Rapid Chloride Ion Permeability of OPC-
31 647 and PPC-Based Carbonated Concrete. *Journal of Materials in Civil
32 648 Engineering*, 24, 606-611.
33
- 34 649 DAS, B. B. & PANDEY, S. P. 2011. Influence of Fineness of Fly Ash on the
35 650 Carbonation and Electrical Conductivity of Concrete. *Journal of Materials in
36 651 Civil Engineering*, 23, 1365-1368.
37
- 38 652 DHIR, R., HEWLETT, P. & CHAN, Y. 1987. Near-surface characteristics of concrete:
39 653 assessment and development of in situ test methods. *Magazine of Concrete
40 654 Research*, 39, 183-195.
41
- 42 655 EL-SAKHAWY, N., EL-DIEN, H., AHMED, M. & BENDARY, K. 1999. Influence of
43 656 curing on durability performance of concrete. *Magazine of Concrete
44 657 Research*, 51, 309-315.
45
- 46 658 ELAHI, A., BASHEER, P. A. M., NANUKUTTAN, S. V. & KHAN, Q. U. Z. 2010.
47 659 Mechanical and durability properties of high performance concretes
48 660 containing supplementary cementitious materials. *Construction and Building
49 661 Materials*, 24, 292-299.
50
- 51 662 EWERTSON, C. & PETERSSON, P. 1993. The influence of curing conditions on the
52 663 permeability and durability of concrete. Results from a field exposure test.
53 664 *Cement and Concrete Research*, 23, 683-692.
54
- 55 665 FATTUHI, N. 1988. Concrete carbonation as influenced by curing regime. *Cement
56 666 and Concrete Research*, 18, 426-430.
57
- 58
59
60
61
62
63
64
65

- 667 FLOWER, D. J. & SANJAYAN, J. G. 2007. Green house gas emissions due to
1 668 concrete manufacture. *The international Journal of life cycle assessment*, 12,
2 669 282-288.
3
- 4 670 GAIMSTER, R. & MUNN, C. 2007. The Role of Concrete in Sustainable
5 671 Development. *Nueva Zelanda*.
6
- 7 672 GOPALAN, M. 1996. Sorptivity of fly ash concretes. *Cement and Concrete*
8 673 *Research*, 26, 1189-1197.
9
- 10 674 GOWRIPALAN, N., CABRERA, J., CUSENS, A. & WAINWRIGHT, P. 1990. Effect of
11 675 curing on durability. *Concrete International*, 12, 47-54.
12
- 13 676 GRUBE, H. & LAWRENCE, C. D. 1984. 'Permeability of Concrete to Oxygen', in
14 677 Proceedings of RILEM seminar on Durability of Concrete Structures under
15 678 Normal Outdoor Exposure, University of Hanover Germany. 68--79
16
- 17 679 GÜNEYISI, E. & GESOĞLU, M. 2008. A study on durability properties of high-
18 680 performance concretes incorporating high replacement levels of slag.
19 681 *Materials and Structures*, 41, 479-493.
20
- 21 682 GÜNEYISI, E., ÖZTURAN, T. & GESOĞLU, M. 2005. A study on reinforcement
22 683 corrosion and related properties of plain and blended cement concretes under
23 684 different curing conditions. *Cement and Concrete Composites*, 27, 449-461.
24
- 25 685 HANEHARA, S., TOMOSAWA, F., KOBAYAKAWA, M. & HWANG, K. 2001. Effects
26 686 of water/powder ratio, mixing ratio of fly ash, and curing temperature on
27 687 pozzolanic reaction of fly ash in cement paste. *Cement and Concrete*
28 688 *Research*, 31, 31-39.
29
30
- 31 689 HAQUE, M. 1990. Some concretes need 7 days initial curing. *Concrete International*,
32 690 12, 42-46.
33
- 34 691 KELHAM, S. 1988. A water absorption test for concrete. *Magazine of Concrete*
35 692 *Research*, 40, 106-110.
36
- 37 693 KHAN, M. & LYNSDALE, C. 2002. Strength, permeability, and carbonation of high-
38 694 performance concrete. *Cement and Concrete Research*, 32, 123-131.
39
- 40 695 KHATIB, J. & MANGAT, P. 1995. Absorption characteristics of concrete as a
41 696 function of location relative to casting position. *Cement and concrete*
42 697 *research*, 25, 999-1010.
43
- 44 698 KHATIB, J. & MANGAT, P. 1999. Influence of superplasticizer and curing on porosity
45 699 and pore structure of cement paste. *Cement and Concrete Composites*, 21,
46 700 431-437.
47
- 48 701 KOCABA, V. 2009. Development and evaluation of methods to follow microstructural
49 702 development of cementitious systems including slags.
50
- 51 703 LAM, L., WONG, Y. & POON, C. 2000. Degree of hydration and gel/space ratio of
52 704 high-volume fly ash/cement systems. *Cement and Concrete Research*, 30,
53 705 747-756.
54
- 55 706 LAWRENCE, P., CYR, M. & RINGOT, E. 2003. Mineral admixtures in mortars: effect
56 707 of inert materials on short-term hydration. *Cement and concrete research*, 33,
57 708 1939-1947.
58
59
60
61
62
63
64
65

- 709 LI, D., CHEN, Y., SHEN, J., SU, J. & WU, X. 2000. The influence of alkalinity on
1 710 activation and microstructure of fly ash. *Cement and Concrete Research*, 30,
2 711 881-886.
3
- 4 712 LO, Y. & LEE, H. 2002. Curing effects on carbonation of concrete using a
5 713 phenolphthalein indicator and Fourier-transform infrared spectroscopy.
6 714 *Building and Environment*, 37, 507-514.
7
- 8 715 MANGAT, P. & EL-KHATIB, J. 1992. Influence of initial curing on sulphate resistance
9 716 of blended cement concrete. *Cement and Concrete Research*, 22, 1089-1100.
10
- 11 717 MEHTA, P. K. 2001. Reducing the environmental impact of concrete. *Concrete*
12 718 *international*, 23, 61-66.
13
- 14 719 MEYER, C. Concrete as a green building material. Construction Materials Mindess
15 720 Symposium, 2005.
16
- 17 721 MEYER, C. 2009. The greening of the concrete industry. *Cement and Concrete*
18 722 *Composites*, 31, 601-605.
19
- 20 723 MOUNANGA, P., KHELIDJ, A., LOUKILI, A. & BAROGHEL-BOUNY, V. 2004.
21 724 Predicting Ca (OH) 2 content and chemical shrinkage of hydrating cement
22 725 pastes using analytical approach. *Cement and Concrete Research*, 34, 255-
23 726 265.
24
- 25 727 NAHATA, Y., KHOLIA, N. & TANK, T. 2014. Effect of Curing Methods on Efficiency
26 728 of Curing of Cement Mortar. *APCBEE Procedia*, 9, 222-229.
27
- 28 729 NASSIF, H. & SUKSAWANG, N. 2002. Effect of curing methods on durability of high-
29 730 performance concrete. *Transportation Research Record: Journal of the*
30 731 *Transportation Research Board*, 1798, 31-38.
32
- 33 732 NATH, P. & SARKER, P. 2011. Effect of fly ash on the durability properties of high
34 733 strength concrete. *Procedia Engineering*, 14, 1149-1156.
35
- 36 734 NEVILLE, A. M. 2011. *Properties of concrete*, Harlow, Prentice Hall.
37
- 38 735 OZER, B. & OZKUL, M. H. 2004. The influence of initial water curing on the strength
39 736 development of ordinary Portland and pozzolanic cement concretes. *Cement*
40 737 *and Concrete Research*, 34, 13-18.
41
- 42 738 PANE, I. & HANSEN, W. 2005. Investigation of blended cement hydration by
43 739 isothermal calorimetry and thermal analysis. *Cement and Concrete Research*,
44 740 35, 1155-1164.
45
- 46 741 PATEL, R., KILLOH, D., PARROTT, L. & GUTTERIDGE, W. 1988. Influence of
47 742 curing at different relative humidities upon compound reactions and porosity in
48 743 Portland cement paste. *Materials and Structures*, 21, 192-197.
49
- 50 744 POON, C., LAM, L. & WONG, Y. 2000. A study on high strength concrete prepared
51 745 with large volumes of low calcium fly ash. *Cement and Concrete Research*,
52 746 30, 447-455.
53
- 54 747 PURNELL, P. & BLACK, L. 2012. Embodied carbon dioxide in concrete: Variation
55 748 with common mix design parameters. *Cement and Concrete Research*, 42,
56 749 874-877.
57
- 58 750 RAMEZANIANPOUR, A. & MALHOTRA, V. 1995. Effect of curing on the
59 751 compressive strength, resistance to chloride-ion penetration and porosity of
60
61
62
63
64
65

- 752 concretes incorporating slag, fly ash or silica fume. *Cement and Concrete*
1 753 *Composites*, 17, 125-133.
- 2
3 754 ROZIERE, E., LOUKILI, A. & CUSSIGH, F. 2009. A performance based approach for
4 755 durability of concrete exposed to carbonation. *Construction and Building*
5 756 *Materials*, 23, 190-199.
- 6
7 757 SABIR, B., WILD, S. & BAI, J. 2001. Metakaolin and calcined clays as pozzolans for
8 758 concrete: a review. *Cement and Concrete Composites*, 23, 441-454.
- 9
10 759 SAKAI, E., MIYAHARA, S., OHSAWA, S., LEE, S.-H. & DAIMON, M. 2005.
11 760 Hydration of fly ash cement. *Cement and Concrete Research*, 35, 1135-1140.
- 12
13 761 SHI, X., XIE, N., FORTUNE, K. & GONG, J. 2012. Durability of steel reinforced
14 762 concrete in chloride environments: An overview. *Construction and Building*
15 763 *Materials*, 30, 125-138.
- 16
17 764 SHOUKRY, S. N., WILLIAM, G. W., DOWNIE, B. & RIAD, M. Y. 2011. Effect of
18 765 moisture and temperature on the mechanical properties of concrete.
19 766 *Construction and Building Materials*, 25, 688-696.
- 20
21 767 SIDDIQUE, R. 2004. Performance characteristics of high-volume Class F fly ash
22 768 concrete. *Cement and Concrete Research*, 34, 487-493.
- 23
24 769 TAN, K. & GJORV, O. E. 1996. Performance of concrete under different curing
25 770 conditions. *Cement and Concrete Research*, 26, 355-361.
- 26
27 771 TASDEMIR, C. 2003. Combined effects of mineral admixtures and curing conditions
28 772 on the sorptivity coefficient of concrete. *Cement and Concrete Research*, 33,
29 773 1637-1642.
- 30
31 774 TEYCHENNÉ, D. C., FRANKLIN, R. E., ERNTROY, H. C., NICHOLLS, J., HOBBS,
32 775 D. & MARSH, D. 1997. *Design of normal concrete mixes*.
- 33
34 776 THOMAS, M. D., MATTHEWS, J. & HAYNES, C. 1989. Effect of curing on the
35 777 strength and permeability of PFA concrete. *Special Publication*, 114, 191-218.
- 36
37 778 TOUTANJI, H., DELATTE, N., AGGOUN, S., DUVAL, R. & DANSON, A. 2004.
38 779 Effect of supplementary cementitious materials on the compressive strength
39 780 and durability of short-term cured concrete. *Cement and concrete research*,
40 781 34, 311-319.
- 41
42
43 782 WANG, P.-M., FENG, S.-X. & LIU, X.-P. 2005. Research Approaches of Cement
44 783 Hydration Degree and Their Development [J]. *Journal of Building Materials*, 6,
45 784 1-10.
- 46
47 785 WHITTAKER, M., ZAJAC, M., HABA, M. B., BULLERJAHN, F. & BLACK, L. 2014.
48 786 The role of the alumina content of slag, plus the presence of additional sulfate
49 787 on the hydration and microstructure of Portland cement-slag blends. *Cement*
50 788 *and Concrete Research*, 66, 91-101.
- 51
52 789 XUE, B., PEI, J., SHENG, Y. & LI, R. 2015. Effect of curing compounds on the
53 790 properties and microstructure of cement concretes. *Construction and Building*
54 791 *Materials*, 101, 410-416.
- 55
56 792 YOUNSI, A., TURCRY, P., AÏT-MOKHTAR, A. & STAQUET, S. 2013. Accelerated
57 793 carbonation of concrete with high content of mineral additions: effect of
58 794 interactions between hydration and drying. *Cement and concrete research*,
59 795 43, 25-33.
- 60
61
62
63
64
65

796

- 1
- 2
- 3
- 4
- 5
- 6
- 7
- 8
- 9
- 10
- 11
- 12
- 13
- 14
- 15
- 16
- 17
- 18
- 19
- 20
- 21
- 22
- 23
- 24
- 25
- 26
- 27
- 28
- 29
- 30
- 31
- 32
- 33
- 34
- 35
- 36
- 37
- 38
- 39
- 40
- 41
- 42
- 43
- 44
- 45
- 46
- 47
- 48
- 49
- 50
- 51
- 52
- 53
- 54
- 55
- 56
- 57
- 58
- 59
- 60
- 61
- 62
- 63
- 64
- 65

Figure 1

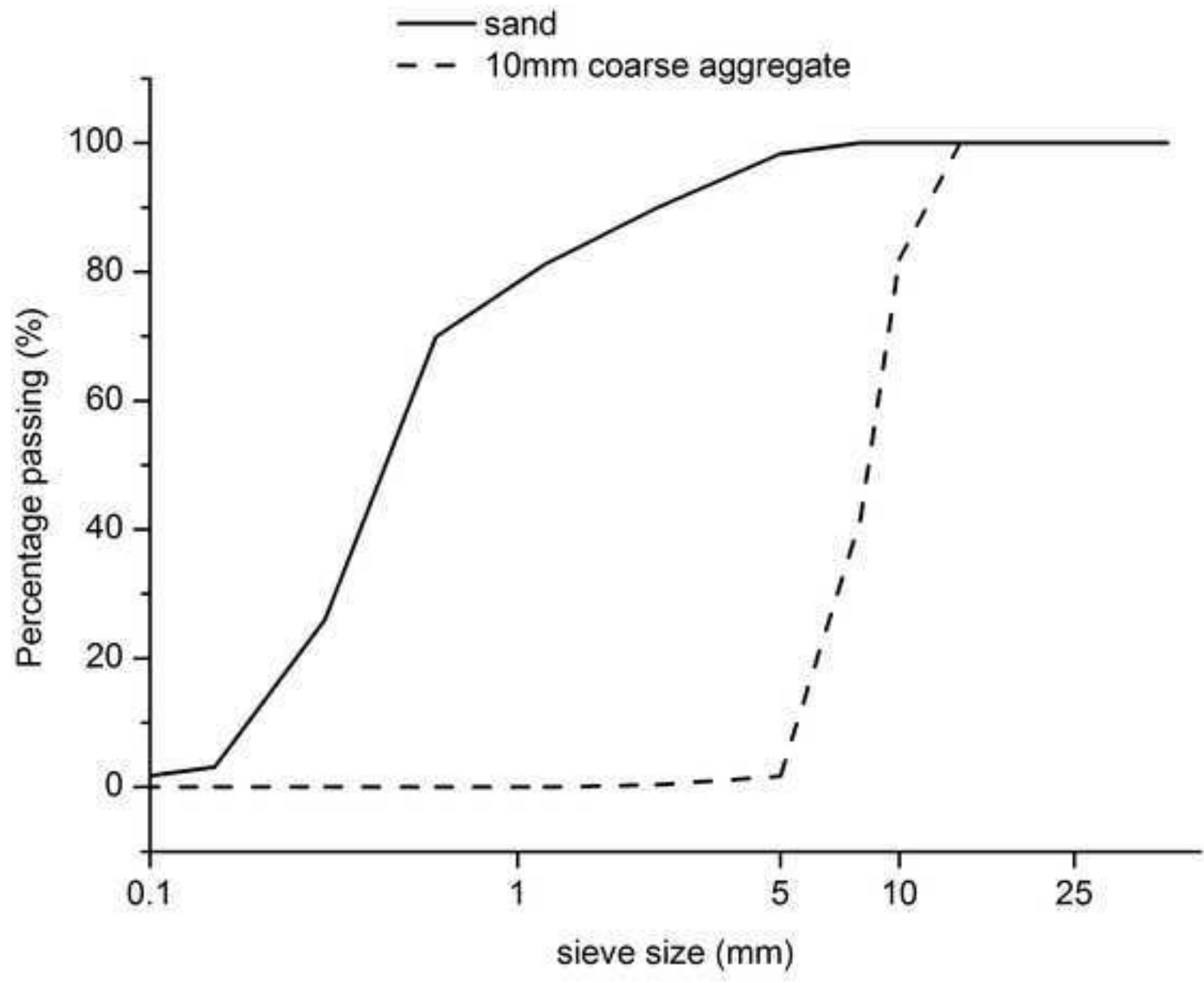


Figure 2



Figure 3

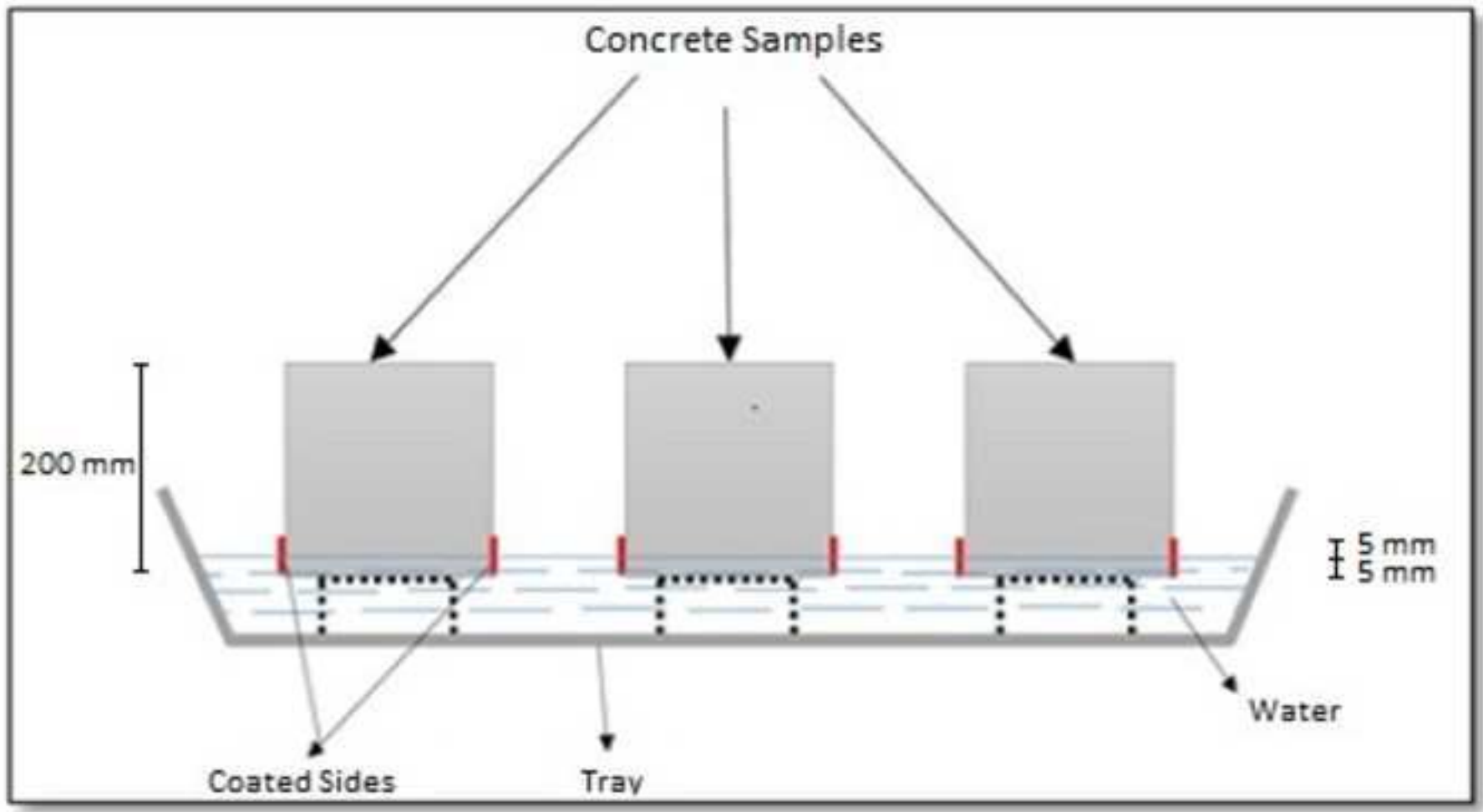


Figure 4

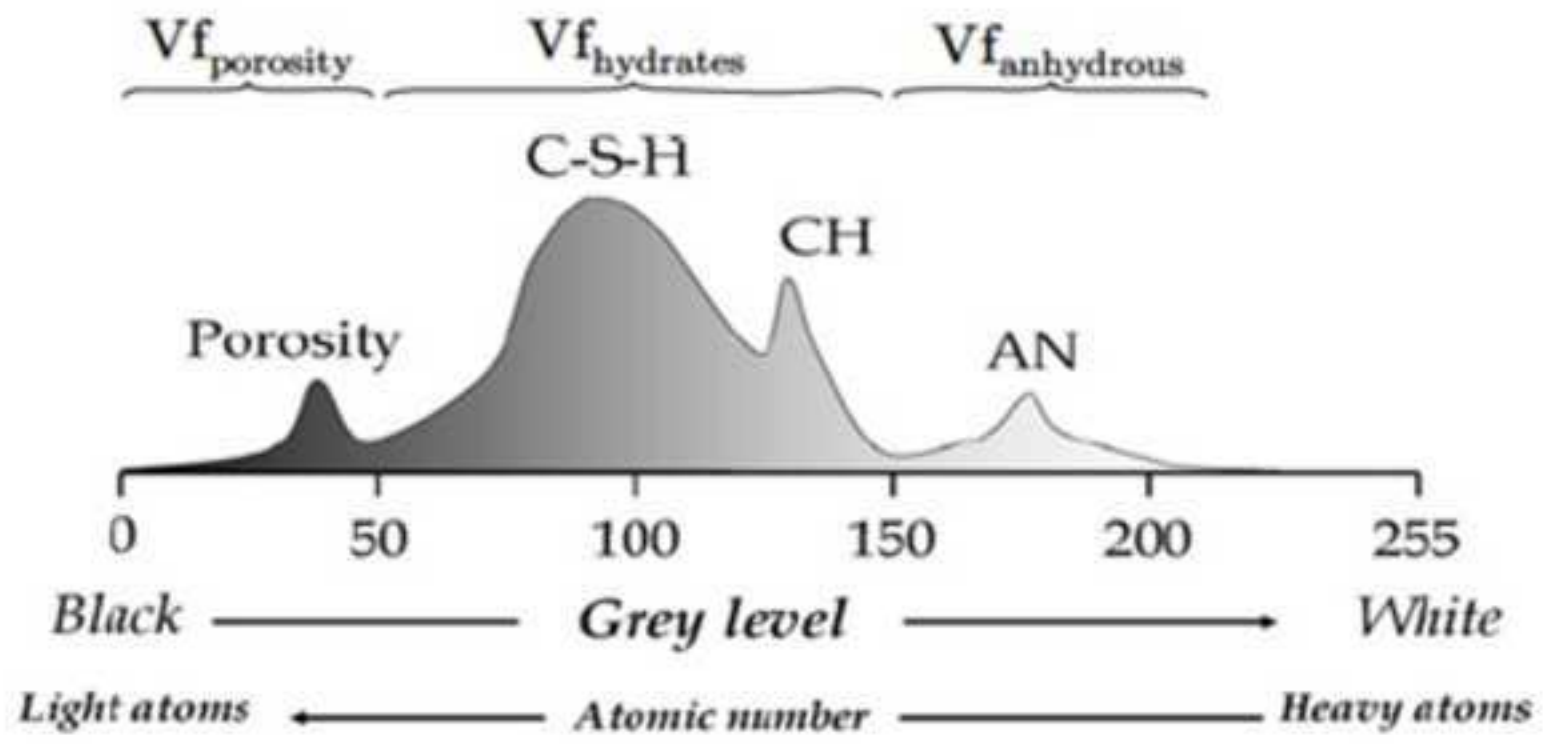


Figure 5

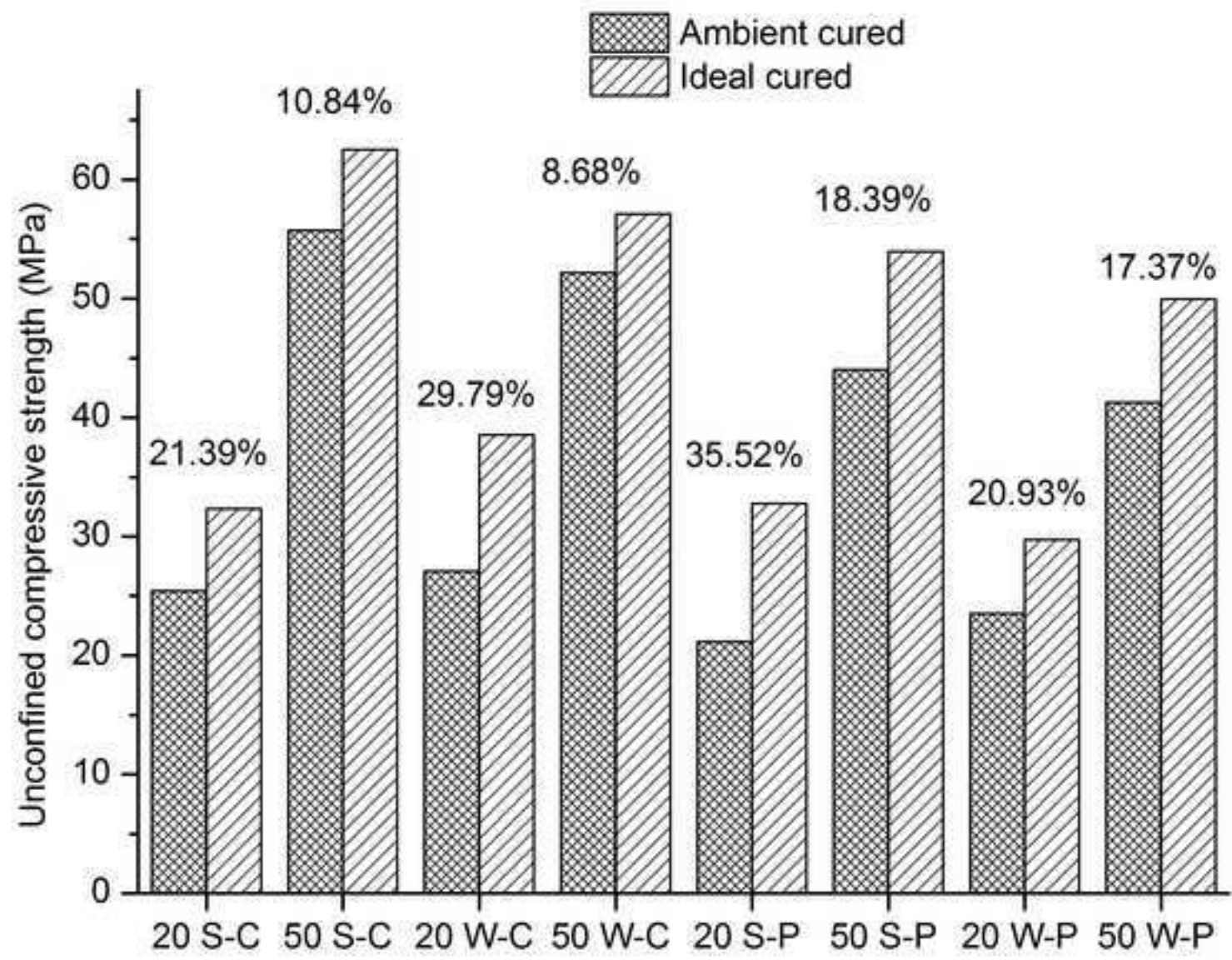


Figure 6

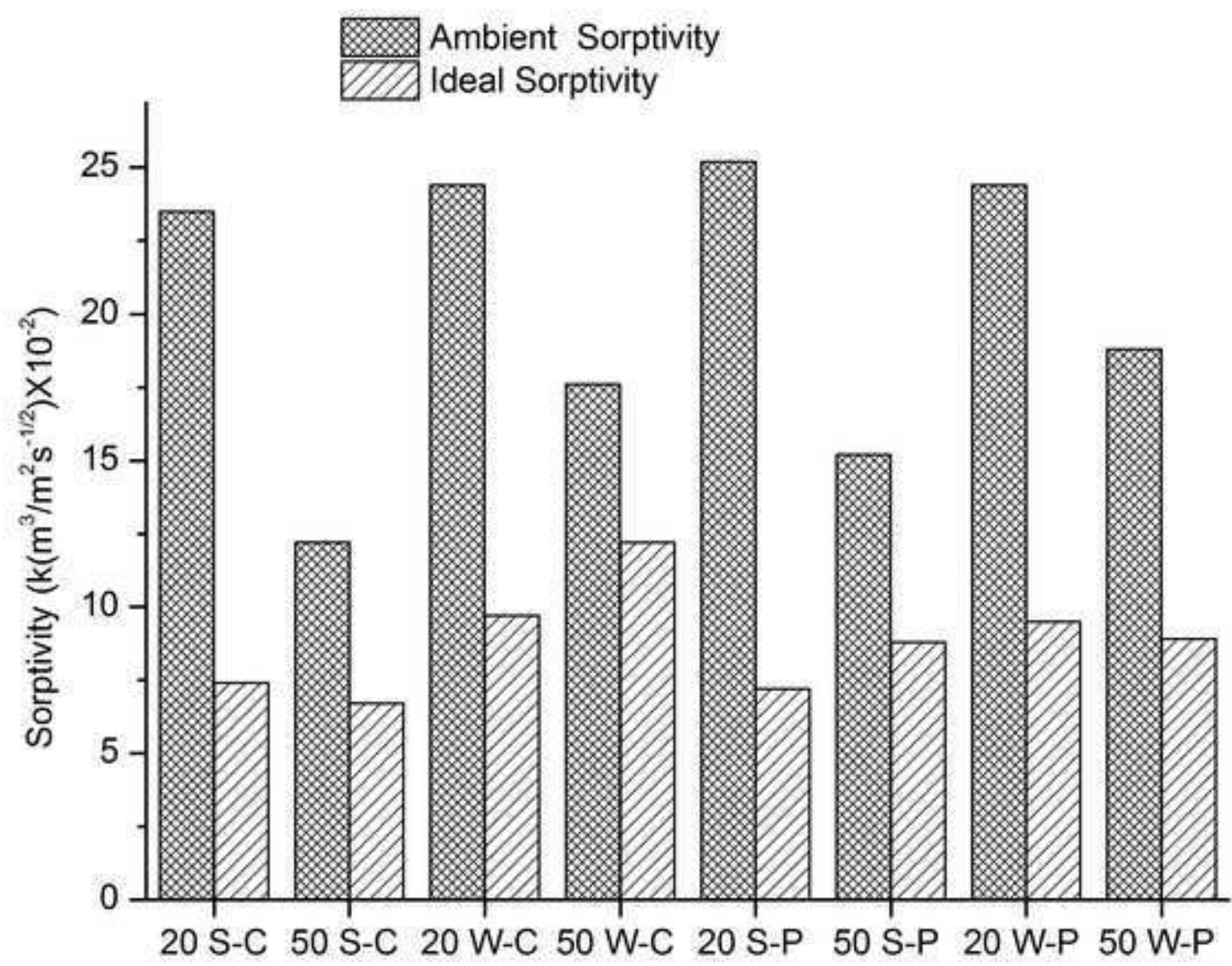


Figure 7

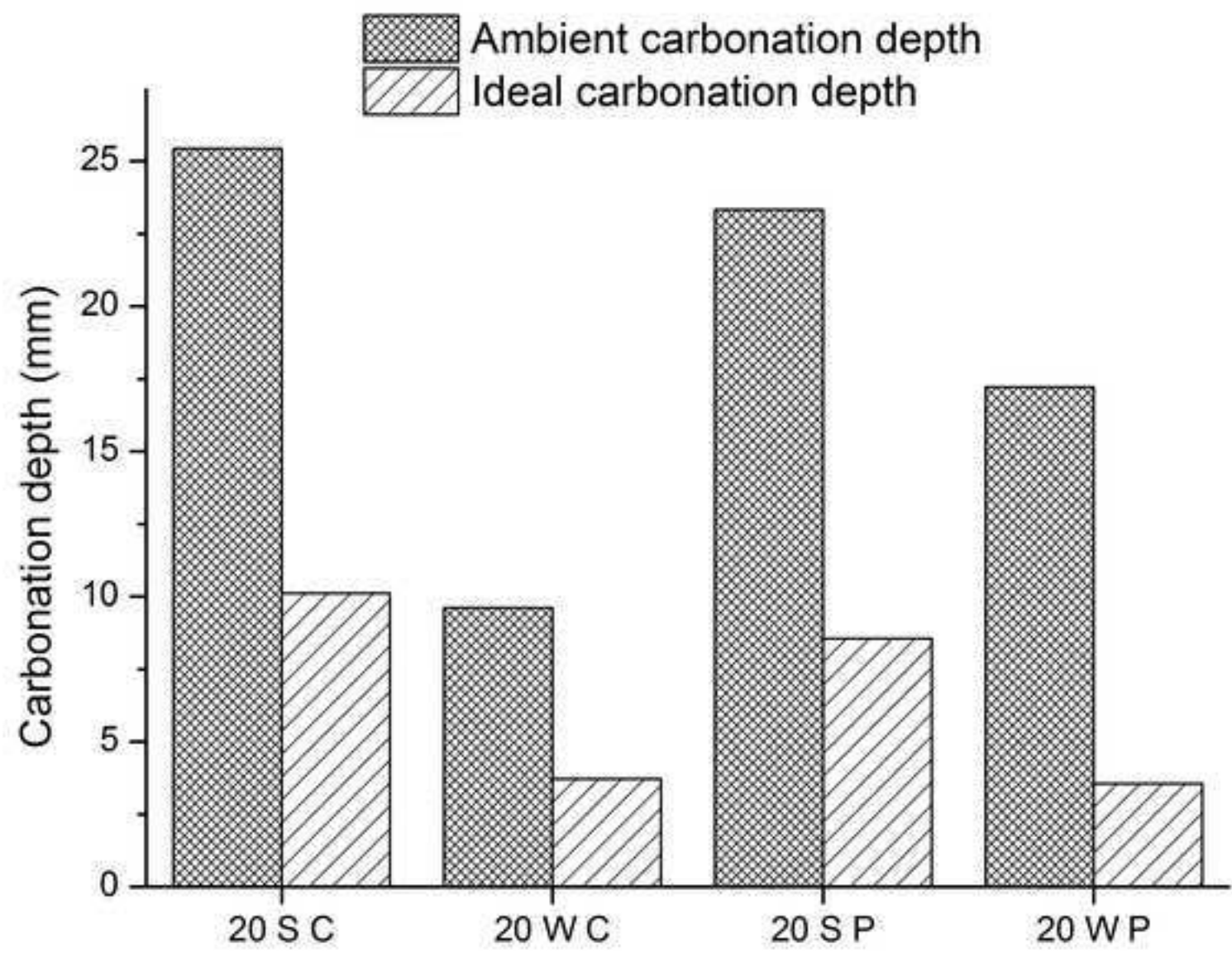


Fig 8a

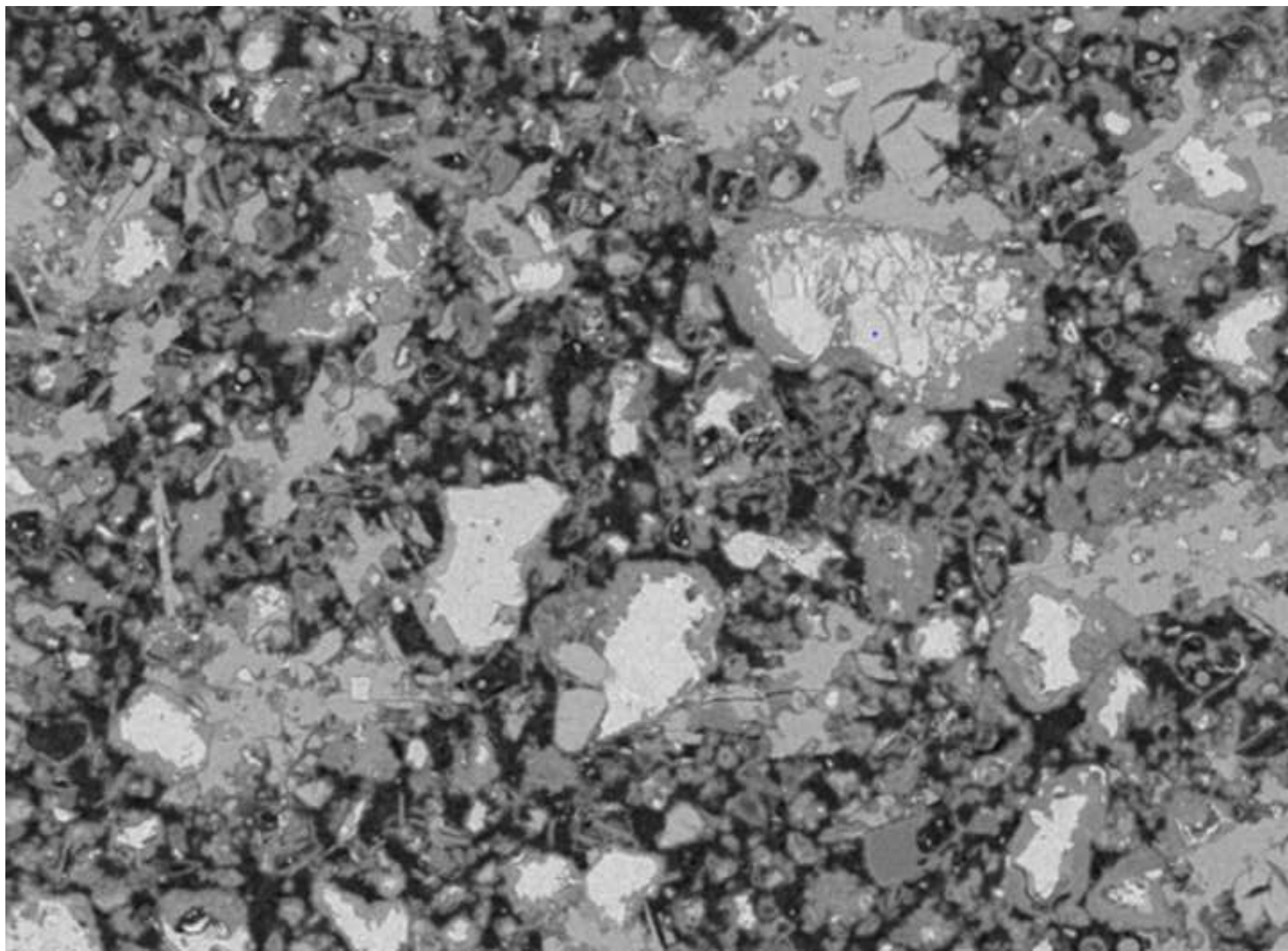


Fig 8b

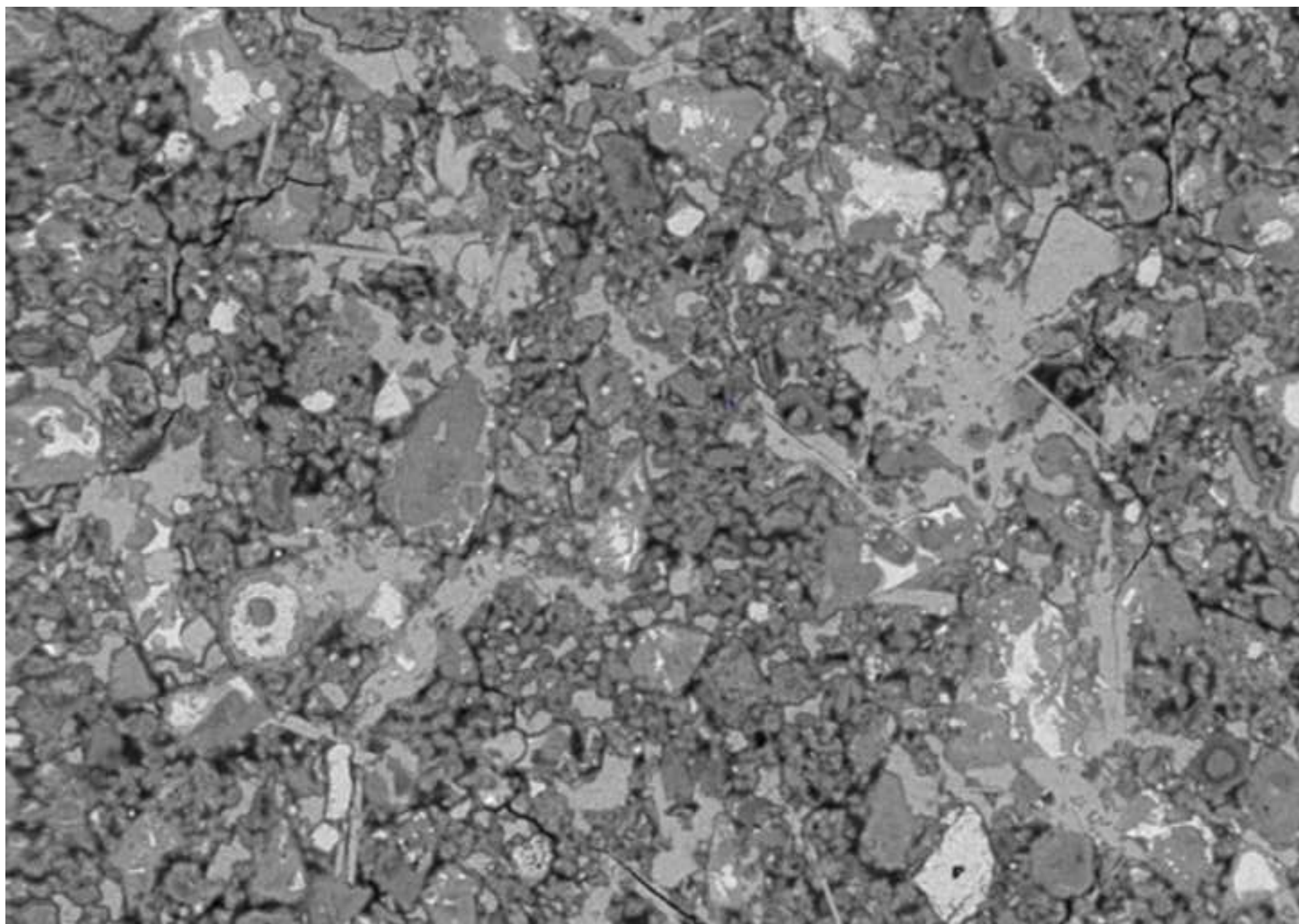


Fig 8c

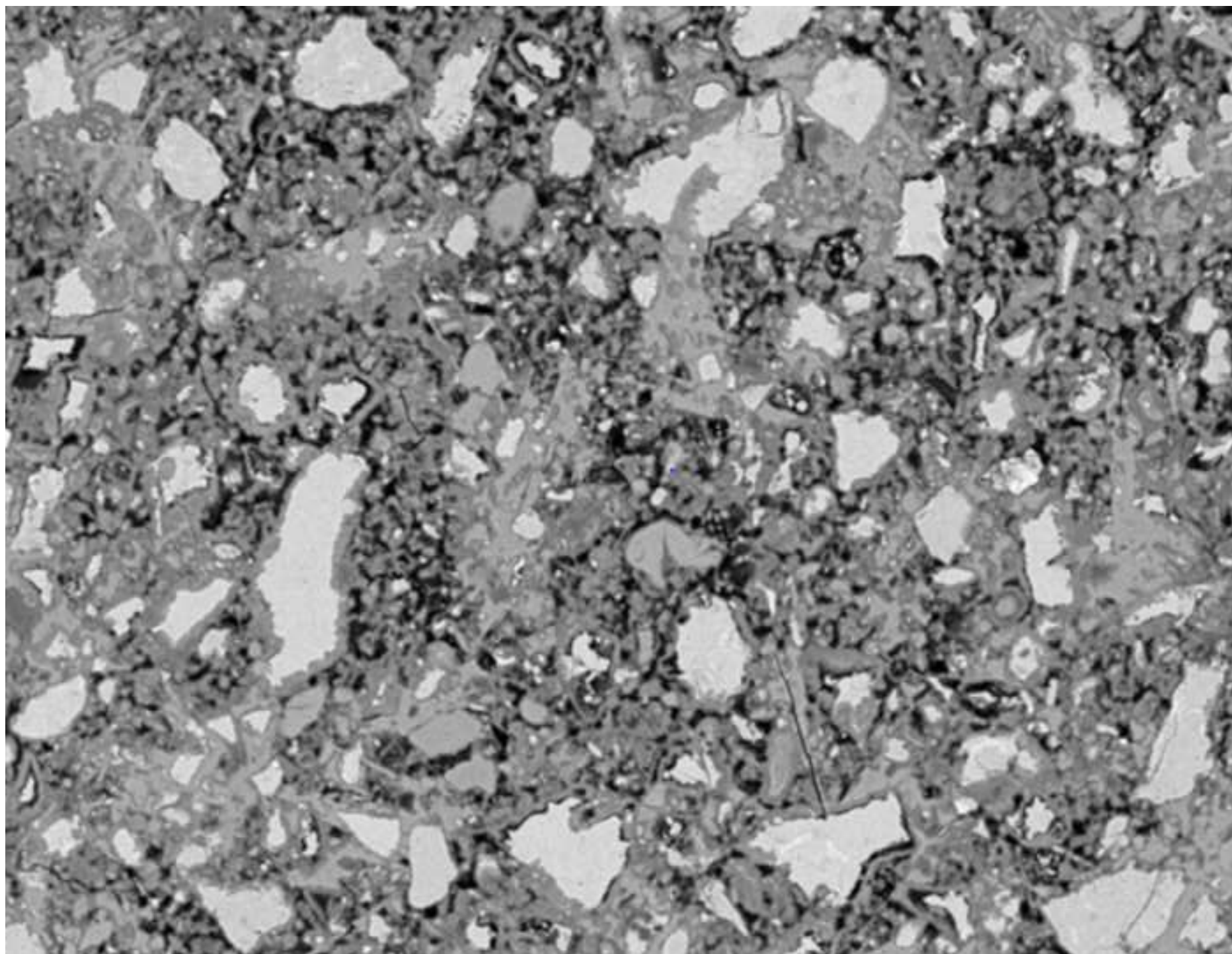


Fig 8d

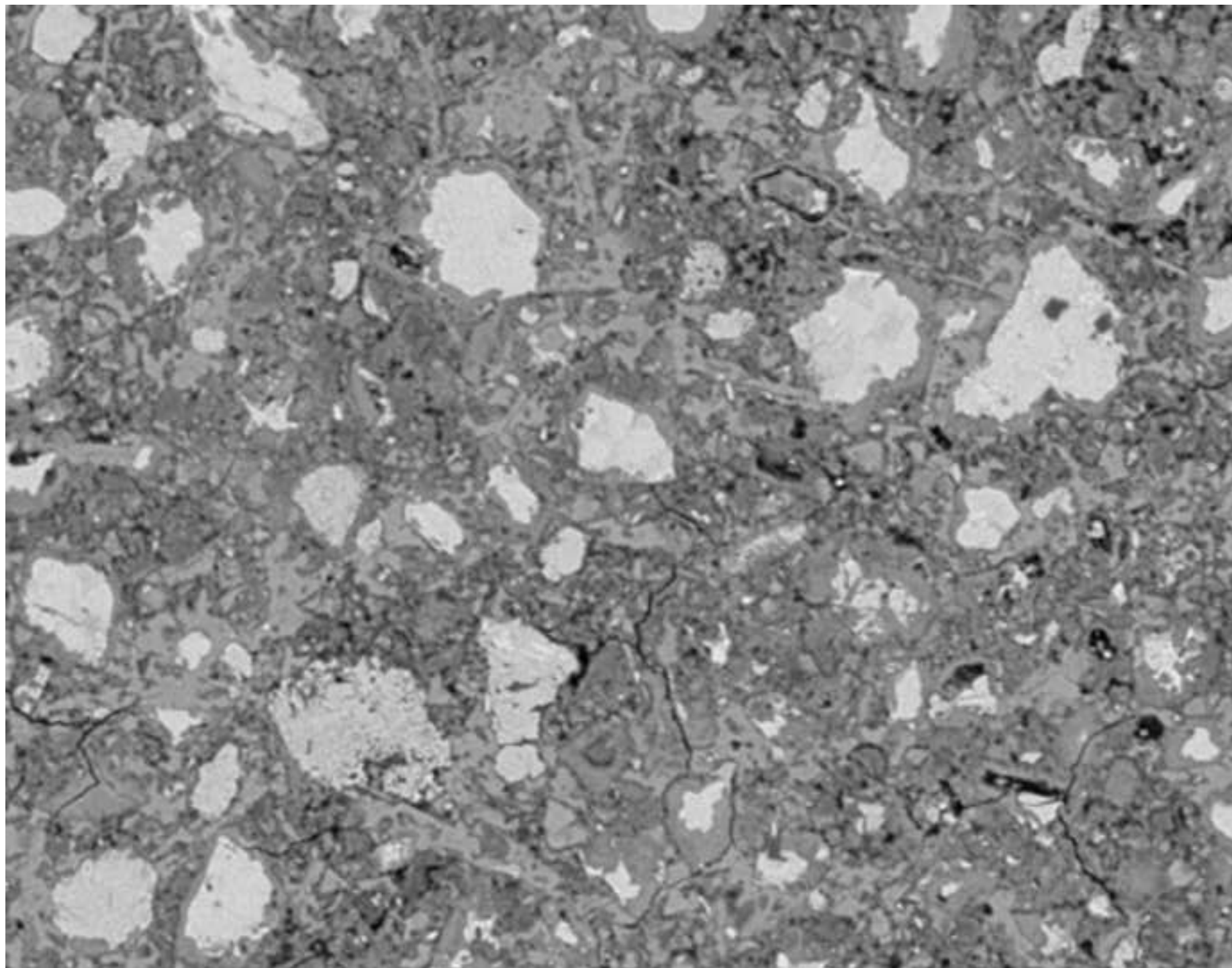


Fig 9a

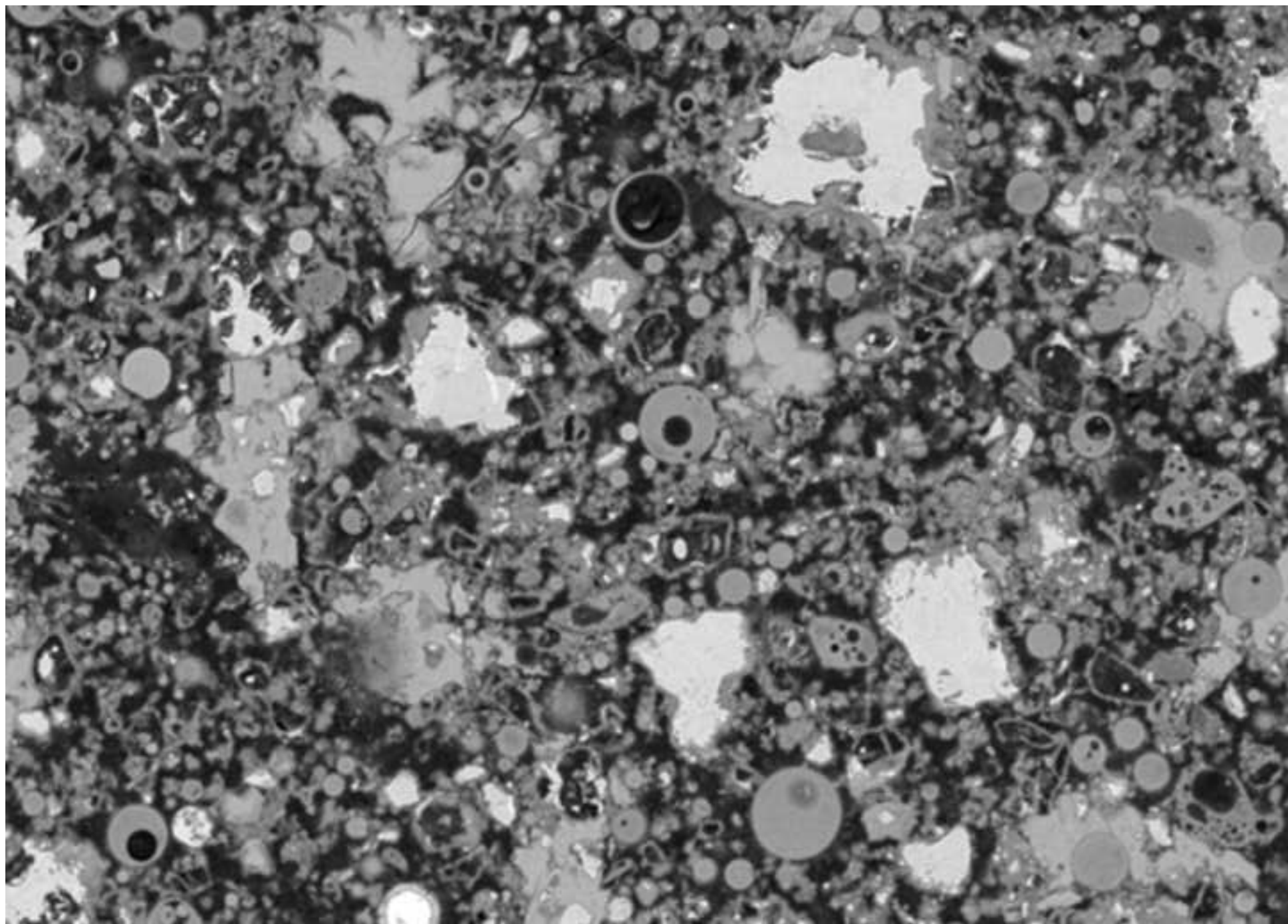


Fig 9b

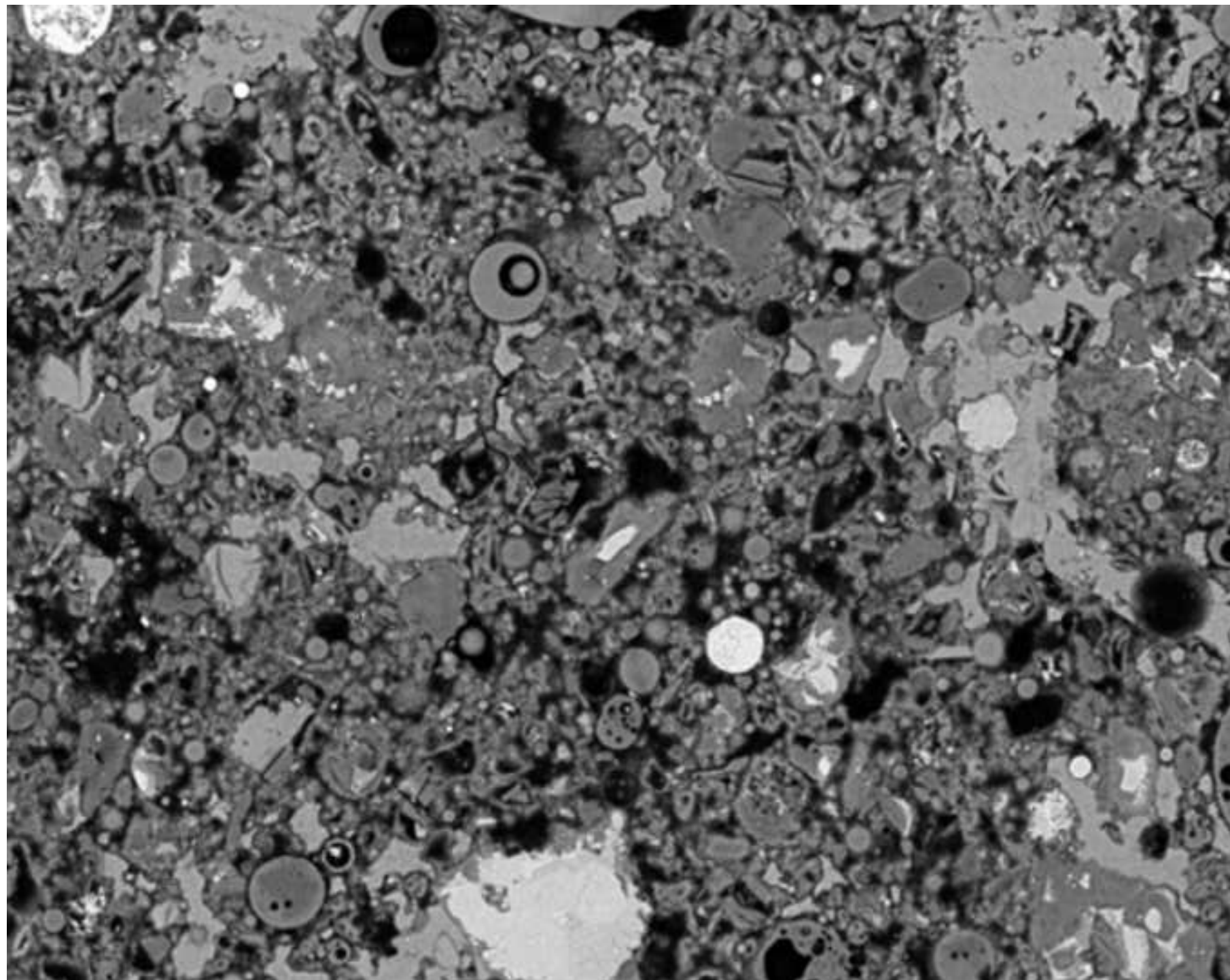


Fig 9c

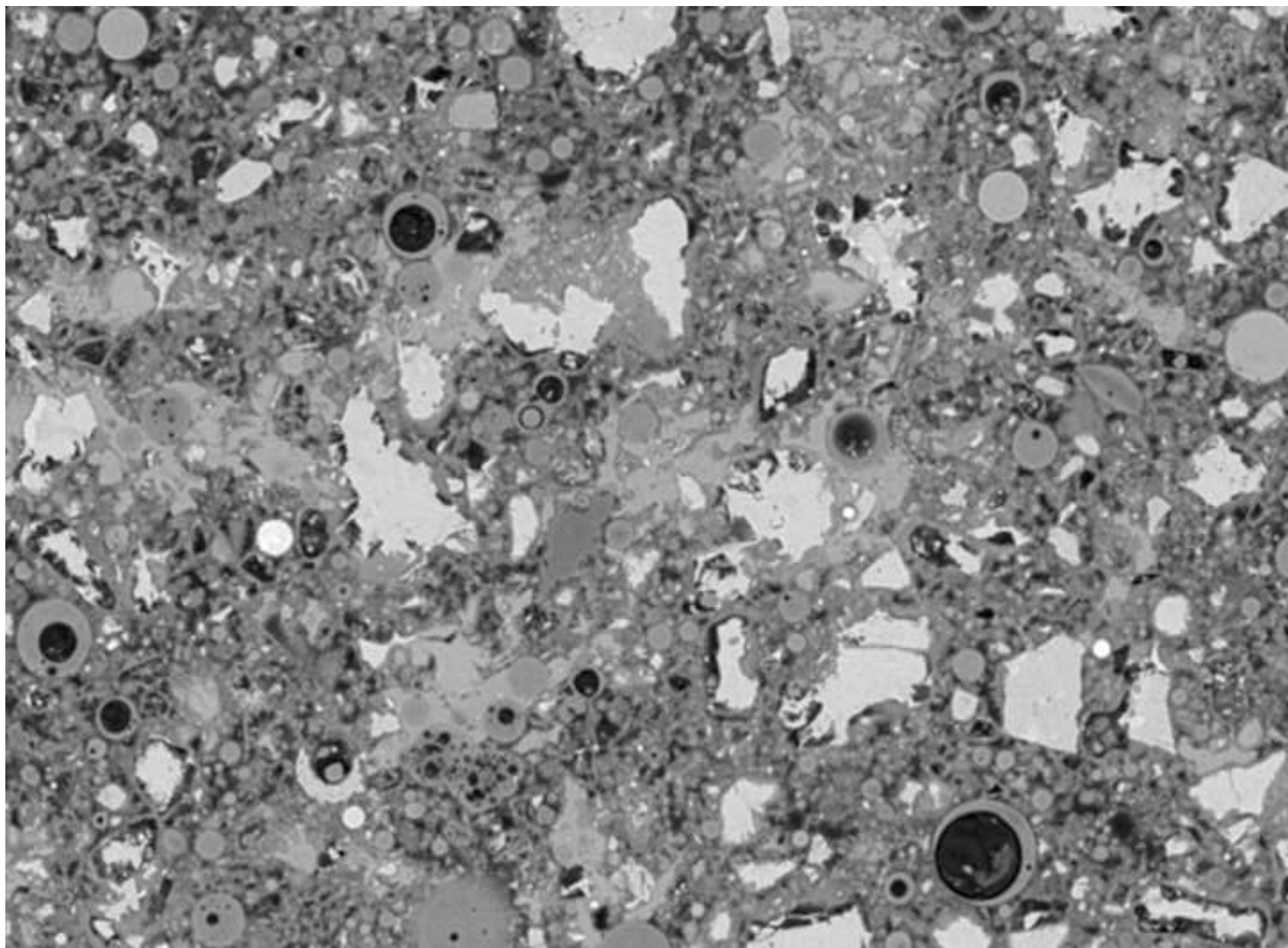


Fig 9d

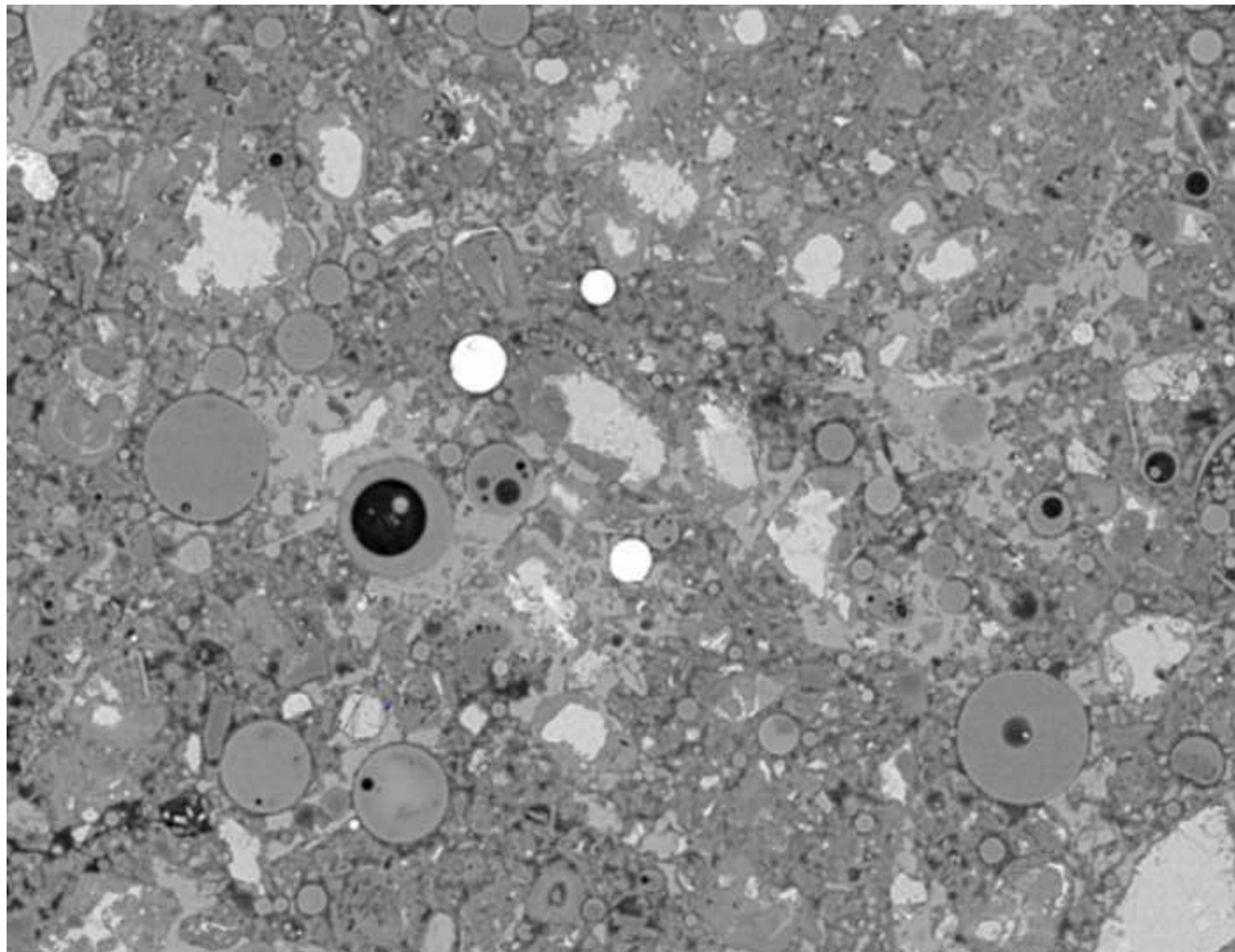


Figure 10

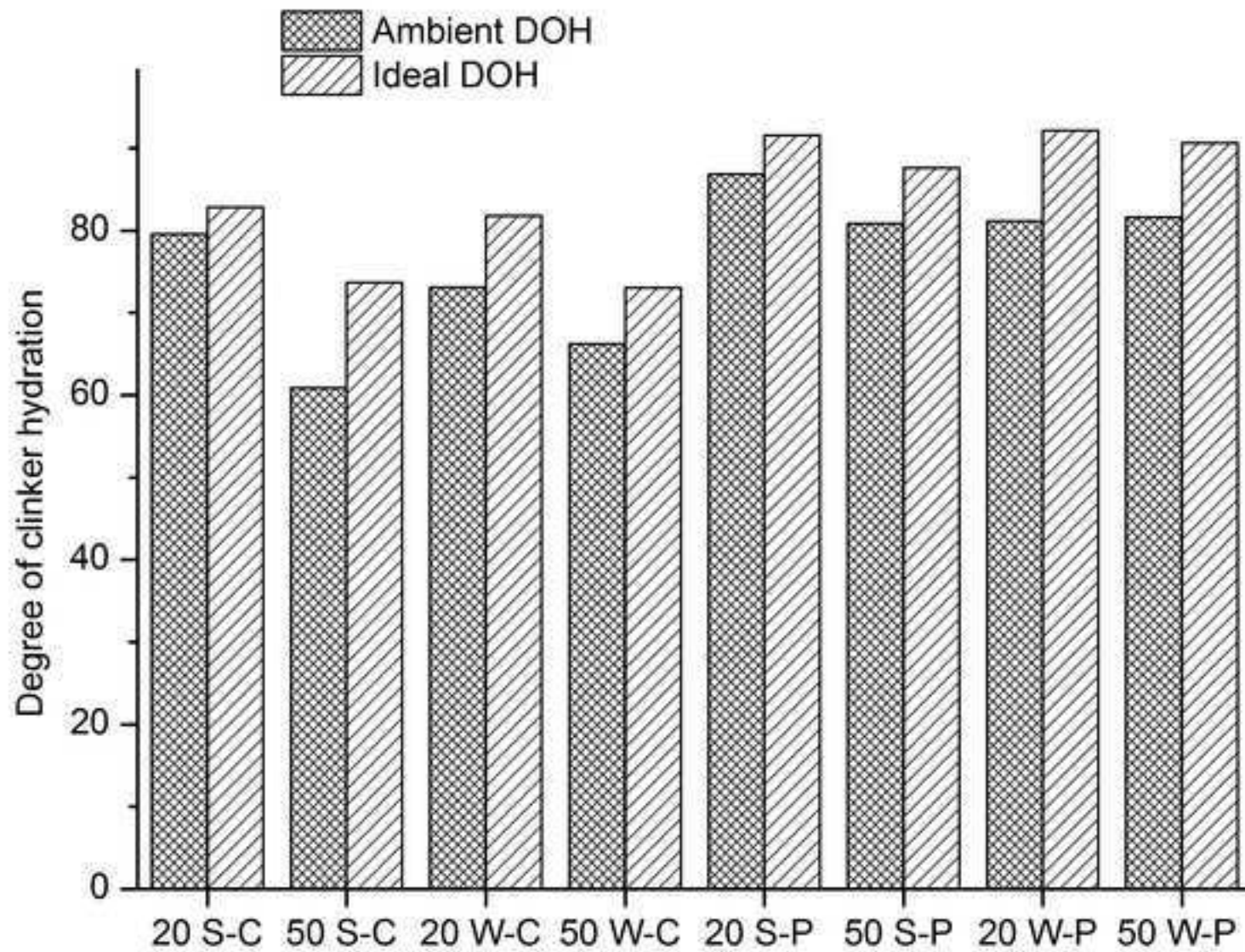


Figure 11

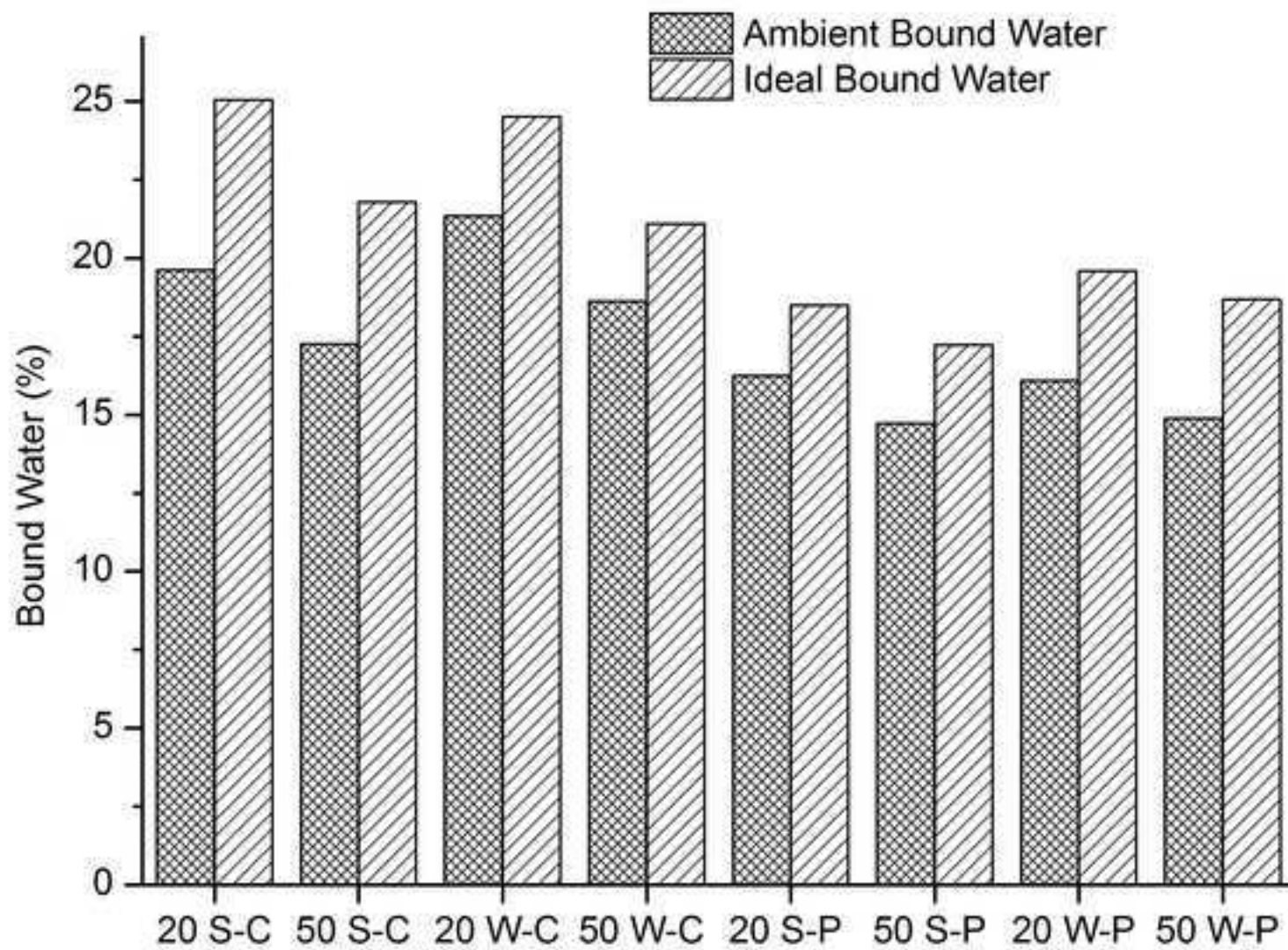


Figure 12

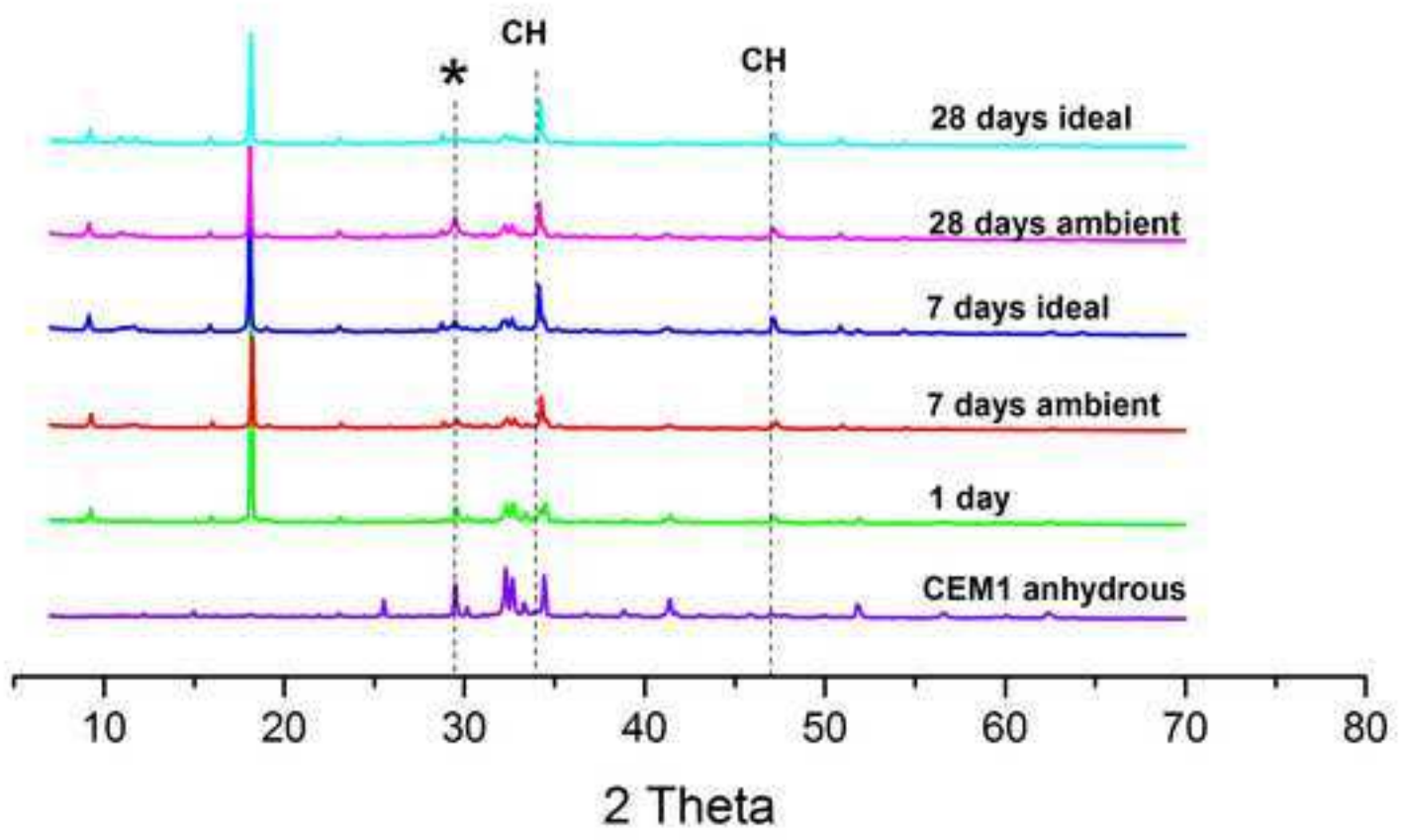


Figure 13

